Early to middle Cenozoic paleoenvironment and erosion estimates of the southwestern Barents Sea: Insights from a regional mass-balance approach

Amando Lasabuda [a,b*], Jan Sverre Laberg [b, a], Stig-Morten Knutsen [c], and Gert Høgseth [a,b]

[a] Research Centre for Arctic Petroleum Exploration (ARCEx), Department of Geosciences, University of Tromsø - the Arctic University of Norway NO-9037 Tromsø, Norway
[b] Department of Geosciences, University of Tromsø - the Arctic University of Norway, NO-9037 Tromsø, Norway
[c] Norwegian Petroleum Directorate (NPD), Harstad, Norway

Corresponding author
E-mail addresses: amando.lasabuda@uit.no, ado.amando@gmail.com

Abstract

The Cenozoic pre-glacial development of the southwestern Barents Sea is discussed, with focus on the early to middle Cenozoic net erosion that was poorly constrained. From 2D and 3D seismic mapping, the western Barents Sea continental margin development shows a complex history of structural configuration of highs and basins related to the Greenland and Eurasian plate movement and subsequent seafloor spreading in the Norwegian-Greenland Sea. Our subdivision of the Sørvestsnaget Basin allows for a closer focus on the tectonostratigraphic development in an overall transtensional setting. To the west, the lower to middle Cenozoic sediments are observed to be systematically overlying the oceanic crust in the Lofoten Basin in accordance to the progressive seafloor's opening. Based on interpretation of five seismic units including sediment progradation (clinoforms) as well as lithology information from exploration wells, the paleoenvironments for the Paleocene, Eocene, Oligocene and Neogene periods were reconstructed. The mass-balance approach has then been used to quantify the corresponding erosion of the southwestern Barents Sea source area. The Stappen High, the Loppa High, and part of mainland Northern Norway are proposed as the key drainage areas covering a combined area of 191,500 to 334,000 km^2, depending on the location of its eastern limit. Our result shows that an average net erosion of 858–1362 m and an average erosion rate of 0.014–0.021 m/k.y have characterized the Cenozoic pre-glacial period. The calculated sediment discharge is 8.7 x 10^6 t/y and the sediment yield is 26.2–45.7 t/km^2/y. Comparison with present-day fluvial systems shows a similar rate of sediment discharge suggesting that our estimates are reasonable. The pre-glacial sedimentation rate is estimated to be 0.026–0.071 m/k.y, which is on average one order of magnitude lower than for the preceding glacial period characterizing this area.

Keywords: southwestern Barents Sea, uplift and erosion, Cenozoic evolution, paleoenvironment, Norwegian Arctic

1. Introduction

Uplift and erosion have affected petroleum basins worldwide and these processes represent major challenges for hydrocarbon exploration (e.g. Knutsen et al., 2000; Henriksen et al., 2011). Moreover, the quantification of the average (net) erosion is an important input for basin modelling in order to estimate the maximum depth of burial of the petroleum system.

In the southwestern Barents Sea, earlier studies addressing uplift and erosion (e.g. Nøttvedt et al., 1988; Vorren et al., 1991; Vågnes et al., 1992; Fiedler and Faleide, 1996; Hjelstuen et al., 1996; Rasmussen and Fjeldskaar, 1996; Dimakis et al., 1998) and recent work utilizing a revised age, a new glaciation model (e.g. Knies et al., 2009; Laberg et al., 2010) and an expanded well database (e.g. Henriksen et al., 2011) have increased our understanding of this topic significantly.

The late Cenozoic glacial erosion, however, does not account for the total net Cenozoic erosion alone. It is likely that there has been a substantial pre-glacial erosion component that also has affected the Barents Sea area as indicated from a considerable amount of Cenozoic sediments overlying the oceanic crust beneath the glacial trough-mouth fans (TMF) (e.g. Vorren et al., 1991; Fiedler and Faleide, 1996). Though, the timing and amount of this erosion is still poorly constrained.

The early to middle Cenozoic evolution of the southwestern Barents Sea continental margin is closely linked to the rifting, breakup and seafloor spreading forming the Norwegian-Greenland Sea (Talwani and Eldholm, 1977; Lundin and Doré, 2002; Tsikalas et al., 2005; Faleide et al., 2008). A shear-dominated setting, episodic magmatic activity, and salt tectonics add to the geological complexity of the margin. Sparse well distribution is also one of the main challenges when reconstructing the regional development of the southwestern Barents Sea area during the Cenozoic.

A mass-balance approach (Doré et al., 2002; Anell et al., 2009; Helland-Hansen et al., 2016) is useful to directly link the offshore deposits to their source area and quantify the amount of erosion, especially for regional studies. This technique has been proven to be useful for the estimation of erosion in the late Cenozoic (e.g. Dowdeswell et al., 2010; Laberg et al., 2012), early–middle Cenozoic (e.g. Lasabuda et al., 2018), and even older systems (e.g. Sømme and Jackson, 2013; Eide et al., 2017). The integration of this method with plate reconstruction will better constrain the dynamic size of the source and sink areas of the southwestern Barents Sea continental margin that was largely affected by the early–middle Cenozoic tectonic.

In this paper, we aim to: 1) describe and discuss the spatial distribution and temporal evolution of the Paleogene–Neogene strata along the southwestern Barents Sea continental margin (to about 74°N) and in the adjacent the Lofoten Basin; 2) discuss the factors that have controlled the development of the succession; and 3) quantify the average erosion and sediment yield of the sediment source areas and discuss the processes involved.

2. Geological setting

The southwestern margin of Barents Sea shelf is characterized by a series of highs and basins (Fig. 1a, b). These predominantly Mesozoic and early to middle Cenozoic highs and basins are related to repeated episodes of continental rifting that are culminated by the NE Atlantic continental separation, and to the onset of sea-floor spreading from early Cenozoic forming the present Norwegian-Greenland Sea (Talwani and Eldholm, 1977; Faleide et al., 1993; Tsikalas et al., 2002; Faleide et al., 2008). In the Middle Jurassic to Early Cretaceous times, an extensional setting governed the tectonic activity (Faleide et al., 2008). Most of the basins of the western Barents Sea shelf experienced various degrees of subsidence. During the Late Cretaceous, the Northern Atlantic realm as well as the southwestern Barents Sea have been dominated by renewed rifting that also affected the Tromsø, Sørvestsnaget, and Harstad Basins (Gabrielsen et al., 1990). The Svalbard Archipelago underwent a more compressional setting and most likely experienced uplift at that time (Bergh et al., 1997).

During the earliest Eocene (from ca. 55 Ma), sea-floor spreading in the Norwegian-Greenland Sea gradually expanded northwards. For the western Barents Sea continental margin, this resulted in the development of a transform setting (Kristoffersen and Talwani, 1977). A major change in plate organization took place in the earliest Oligocene time (ca. 33 Ma) when the Greenland plate started to move in the same direction as the North American plate (Kristoffersen and Talwani, 1977; Faleide et al., 1993). In the Norwegian-Greenland Sea, this event resulted in a readjustment of the relative seafloor spreading motion from NNW-SSE to NW-SE (Faleide et al., 2008).

The transform system of the western Barents Sea continental margin occurred at an angle to the spreading axis that created segmentation over a large area (Faleide et al., 1993). The Senja Fracture Zone and the Hornsund Fault Zone are the two large shear segments of this transform separated by the Vestbakken volcanic province as the central segment (Fig. 1c). To the south, the Senja Fracture Zone experienced dextral oblique shear that resulted in an overall transtensional regime of the Sørvestsnaget Basin (Faleide et al. 1993, Kristensen et al. 2017). The transtension mechanism has been explained by strain partitioning into shortening and extension that formed coevally, particularly in the southern and central part of the Sørvestnaget Basin (Kristensen et al., 2017). To the northeast, part of the Stappen High was part of the Cretaceous Bjørnøya Basin before it was inverted in the early Cenozoic (Blaich et al., 2017). However, in the northwestern part, the transition from the Sørvestsnaget Basin towards the Vestbakken volcanic province is less understood.

The Vestbakken volcanic province (Gabrielsen et al., 1990) marks the relay zone with significant volcanism and lava intrusion in a pull-apart basinal setting (Faleide et al., 2008) (Fig. 2). The Eocene rifting included the extensional faulting in the Knølegga Fault Complex. Possible fault reactivation in the earliest Oligocene (Eidvin et al., 2014) may contribute to a regional compression event (Blaich et al., 2017). Moreover, widespread salt diapirs in the Sørvestsnaget and Trømsø Basins are suggested to be developed in the early Cenozoic and have affected the tectonosedimentary style in those basins (Perez-Garcia et al., 2013).

Parts of the Hornsund Fault Zone near Svalbard appeared to have been compressed during the Paleocene–Eocene transition, later becoming a sheared margin and subsequently rifted in the Oligocene (Lundin and Doré, 2002; Bergh and Grogan, 2003). Significant parts of Svalbard were uplifted due to crustal shortening and subsequent exhumation, which caused it to be the most eroded part in the wider Barents Sea (Faleide et al., 2008; Henriksen et al., 2011). This early Cenozoic event resulted in the formation of West Spitsbergen Fold-Thrust Belt and the development of the Central Basin as a foreland basin to the east (e.g. Braathen et al., 1995; Bergh et al., 1997).

During the Plio–Pleistocene, multiple phases of glacial development have been identified in the Barents Sea area (Knies et al., 2009). During the glacial maxima, large quantities of sediments were eroded from the land and/or shallow shelf areas and deposited along the deeper continental shelf and slope. Laberg et al. (2010) interpreted the paleoenvironment in the early stage as dominated by glaciofluvial processes of erosion and sediment transport. Later, subglacial erosion and deposition of deformation till beneath and in front of fast-flowing ice streams were the most important processes. The glacial erosional product deposited along the continental slope led to the development of the Bear Island TMF (Laberg and Vorren, 1993, 1995; Faleide et al., 1996; Fiedler and Faleide, 1996; Laberg and Vorren, 1996).

3. Cenozoic uplift and erosion

The present-day morphology and depth of the southwestern Barents Sea is suggested to be a result of several episodes of Cenozoic uplift and erosion. Different approaches have been applied to estimate the timing and to quantify the erosion in the southwestern Barents Sea (Cavanagh et al., 2006; Henriksen et al., 2011). The results of these studies, including estimates of the erosion for each period, are summarized below.

3.1. Estimates of the total net erosion

Net erosion is defined as the total difference between the maximum burial and the current depth of a succession (Riis and Jensen, 1992; Doré and Jensen, 1996). Henriksen et al. (2011) compiled a Cenozoic net erosion map for the wider Barents Sea area based on weighted-average results from well data including vitrinite reflectance, sandstone diagenesis, apatite fission track, and shale compaction. They estimated that the net erosion affecting the sedimentary basins of the southwestern Barents Sea is between 900 to 1400 m. Recently, Ktenas et al. (2017) presented an updated net erosion map for the southwestern Barents Sea area based on sonic velocities and shale-sand compaction trends with higher values of net erosion, 1400–1750 m for most of the area south of ~72°30’N and east of 18°E. Baig et al. (2016) using shot gathers, well logs, and thermal maturity data suggested maximum values of average net erosion of up to 1950 m and 2100 m for the Loppa High and the Stappen High areas, respectively. Furthermore, studies from Bjørnøya (the exposed part of the Stappen High) show that up to 3000–4200 m of net erosion has affected this area (Wood et al., 1989; Ritter et al., 1996).

3.2. Estimates of the glacial erosion

An important part of the net erosion was due to glacial erosion from the Barents Sea Ice Sheet repeatedly covering the Barents Sea shelf during the Pleistocene (e.g. Laberg et al., 2012). The western Barents Sea continental slope and the Lofoten Basin are identified to have been the main depocenter of the eroded Barents Sea shelf sediments (Fig. 1b). Here, the thick, prograding Pleistocene wedges / trough-mouth fans (TMF) are the prominent features (i.e. the Bear Island and Storfjorden TMFs). These TMFs comprise three main seismic units, GI–GIII of Faleide et al. (1996) or TeC–TeE of Vorren et al. (1991). From estimates of the sediment volume of these units, their inferred age and source area (the mass-balance approach), the total erosion and erosion rate have been estimated (Fiedler and Faleide, 1996; Hjelstuen et al., 1996; Laberg et al., 2012). Alternative approaches have been presented by using present-day bathymetry (Rasmussen and Fjeldskaar, 1996) and vitrinite reflectance, shale compaction, geochemical analysis, and seismic velocities (Dimakis et al., 1998).

Laberg et al. (2012) presented a revised estimate of the glacial erosion and deposition of the southwestern Barents Sea area using the mass-balance method. Their main findings can be summarized as follows: 1) A period of pre-glacial, mainly glaciofluvial erosion from ~2.7–1.5 Ma with a total erosion of 170–230 m, an average erosion rate of 0.15–0.2 mm/yr, and an average sedimentation rate of 16–22 cm/ky were found. 2) The total erosion during the period from ~1.5–0.7 Ma was in a range of 330–420 m with an average erosion rate of 0.4–0.5 mm/yr. The average sedimentation of 50–64 cm/ky was higher than for the previous period. This period was likely dominated by subglacial erosion beneath paleo-ice streams including glaciotectonism. 3) The most pronounced but more spatially restricted glacial erosion occurred during the last 0.7 Ma, with a total erosion of 440–530 m in the glacial troughs of the shelf. The average erosion is estimated to be 0.6–0.8 mm/yr and the average sedimentation rates were 18–22 cm/k.y.

In a more recent study, Zieba et al. (2016) modelled the Pleistocene glacial erosion and found that in this period the erosion was small. This is most likely related to the location of their study area, in the outer part of Bjørnøyrenna which was less affected by erosion compared to the inner (eastern) part. Their findings are in agreement with the general stratigraphy development of this area where units GI and GII were dominated by erosion, while unit GIII was dominated by aggradation (e.g. Laberg et al., 2010).

The impact of glacial erosion was more dominated in the troughs compared to the bank areas (see Laberg and Vorren, 1995). This is due to the presence of the fast-flowing ice streams in the troughs that erodes more effectively than the ice in the banks (e.g. Laberg et al., 2010) However, in the average glacial erosion estimates using the mass-balance approach, spatial variations were not accounted for (Laberg et al., 2012). Recent studies by Zattin et al. (2016) and Zieba et al. (2016) document that there were local variations of glacial erosion including the westernmost part of the southwestern Barents Sea shelf (outer Bjørnøyrenna) were the erosion was relatively low. This shows that the combination of regional mass-balance studies and more local studies from well data is useful to capture the spatial variation of glacial erosion reflecting the dynamics of the Barents Sea Ice Sheet.

Zieba et al. (2017) modelled early Pleistocene bathymetry of the southwestern Barents Sea area and found it to have been close to sea level with some areas elevated to about 300 m. Their result is in conformity with and refine previous results suggesting that the Barents Sea was at or near sea level or even partly subaerially exposed prior to glaciation (e.g. Vorren et al., 1991; Butt et al., 2002 and references therein).

3.3. Estimates of the pre-glacial erosion

Few studies have specifically addressed pre-glacial estimates. Using the mass-balance approach, Vorren et al. (1991) and Fiedler and Faleide (1996) mapped and studied the Cenozoic pre-glacial sediments in the Lofoten Basin. Fiedler and Faleide (1996) estimated an average minimum net pre-glacial erosion of approximately 562 m for the southwestern Barents Sea. Following the study by Vorren et al. (1991), Richardsen et al. (1993) concluded that 600–1200 m of erosion must have occurred in the southwestern Barents Sea during the Eocene, Oligocene, and Miocene.

4. Data and methods

The seismic data consist of 2D and 3D seismic datasets (NH-803 and EL0001) (Fig. 4). The seismic data were provided by the Norwegian Petroleum Directorate (NPD) and TGS/Spectrum. The 3D seismic data have an average interval velocity of 2.1 km/s and dominant frequency of 20 Hz for the studied succession, therefore, the vertical resolution is about 26 m (Safronova et al. 2012). This interval velocity was used to convert fault displacement in the Sørvestsnaget's sub-basins. The normal polarity standard of Society of Exploration Geophysicist (SEG) has been applied (Sheriff, 1991). The seismic data are of good quality in most of the study area.

Seismic stratigraphic interpretation including horizon and fault mapping was the main tool for establishing and characterizing the structural and stratigraphic framework. The bounding reflections, internal seismic signatures and unit geometries were then described for the five seismic units bounded by six key horizons (Fig. 2). The seismic stratigraphy concept of Mitchum Jr et al. (1977) has been applied. Seven wells with NPD welltops have been used to tie the seismic data as an age control on the stratigraphic framework (Fig. 1c). The geological timescale of Cohen et al. (2016) was used in this study. The time-to-depth value of 2.68 km/s documented by Fiedler and Faleide (1996) was applied, as their results were closely similar to the trendline equation from checkshot data from the relevant wells for this study (Fig. 3).

In order to quantify the amount of erosion affecting the southwestern Barents Sea area during early to middle Cenozoic, the volumetric mass-balance method (also referred to as the source-to-sink method) was used (e.g. Laberg et al., 2012). The results are presented as isopach maps showing the distribution and thickness of the studied succession. The isopach maps were created following True Stratigraphic Thickness (TST) between top and base surfaces. By calculating the sediment volume of the basin deposits, we can estimate the volume of the erosional products of the drainage area using the mass-balance approach. GPlates v. 2.0 software (Matthews et al., 2016; Müller et al., 2016) was used to constrain the size of the Cenozoic basins and the relative position of plates.

In the mass-balance approach, the volume of the deposited sediment is assumed to be the same as the volume eroded from the source area after some corrections have been applied. Furthermore, the location of their likely source area are indicated by the sediment progradation pattern. From this, sedimentation rate and corresponding total erosion and erosion rate are calculated and discussed. For source area, we use the term erosion for describing a surficial removal of mass by any kind of weathering (mechanical, chemical, and biological) for both subaerial and submarine settings (Riis and Jensen, 1992; Doré et al., 2002; Leeder, 2009). Erosion is measured as an effect on the surface, whereas denudation includes subsurface processes. Here we do not account for mass dissolution, therefore, we do not consider denudation (see Lasabuda et al., 2018). Moreover, erosion estimates addressed here are considered as a long term erosion and average values, whereas erosion rates can be highly variable over time.

5. Results

The study area is divided into two main parts, the eastern and the western part (Fig. 4). The eastern part consists of a series of highs and basins within the southwestern Barents Sea shelf. The sediment deposited in the eastern part is regarded as the accumulation in the continental margin sink. The western part is the Lofoten Basin and is regarded as the oceanic basin sink.

The structural and stratigraphic frameworks of the southwestern Barents Sea, primarily the Sørvestsnaget Basin, are presented first. Then, the deposits in the Lofoten Basin are included.

The seismic units are described along with their seismic character and thickness variation. Then, isopach maps are presented for each seismic unit. These form the basis for sediment yield calculation in order to quantify the rate of erosion and sedimentation.

5.1. Continental margin sink: Sørvestsnaget Basin subdivision

In this study, the Sørvestsnaget Basin is divided into 4 sub-basins reflecting the complex geometry of this area. They are named Sub-basins A to D, located from north to south (Fig. 1c). The sub-basins are all bounded by a system of major normal faults on one side (east) and smaller antithetic faults to the west (Figs. 5–7). The major extensional fault systems (Faults 1–5) have affected most of the pre-glacial Cenozoic sediment and are interpreted as the pre- to syn-depositional fault system. The faults show a broad NE-SW trend and penetrate the deeper (Cretaceous) strata.

5.1.1. Sub-basin A

Sub-basin A is located in the north-westernmost part of the Sørvestsnaget Basin (Fig. 1c). Fault 1 is part of the southeasterly dipping extensional fault system that separates this sub-basin from the Vestbakken volcanic province to the north. The key observation that allows for this sub-basin to be considered as part of the Sørvestsnaget Basin is that there is no apparent high amplitude reflections indicating volcanic deposits (Figs. 5 and 6). Fault 1 terminates upwards within the lower Eocene succession and is interpreted as an antithetic fault related to a series of fault to the southeast (Fig. 5). A displacement from ca. 200 to 500 ms TWT (two-way travel time) (ca. 210 to 525 m) is observed at the base of the Paleocene (Fig. 6).

In its axial part, Sub-basin A is characterized by a series of NE trending extensional faults that shows a growth into the Oligocene–Neogene interval (Fig. 5). In planar view, these faults are densely spaced and have lengths of up to ca. 25 km. Sub-basin A narrows in width towards the Senja Fracture Zone to the south and marks the transition to the oceanic crust to the west (Fig. 1c). Towards Sub-basin B, Sub-basin A is bounded by Fault 2 that resulted in the formation of the intrabasinal high (Ryseth et al., 2003), an apparent continuation of the marginal high (Fig. 1c). Fault 2 is regarded as the southwestward continuation of the Knølegga Fault Complex. This major fault is a steeply dipping fault with more than 250 ms (ca. 260 m) throw at deeper Cretaceous strata, indicating that the fault was part of the rifting during the Cretaceous (Figs. 5 and 6).

5.1.2. Sub-basin B

Sub-basin B is situated immediately west of the Bjørnøya Basin which are separated by a set of extensional faults (Fig. 1c). These NW-SE striking faults are up to ca. 35 km long and represent NE-SW oriented extension. Sub-basin B is separated from the intrabasinal high by a set of antithetic faults (Fig. 6). These minor faults show typically 100–200 ms (ca. 105–210 m) displacements at the base of the lower Eocene. The structural style is interpreted as a series of tilted fault blocks with increasing thickness in the lower Eocene interval.

Fault 3 marks the boundary to Sub-basin C and is a segmented NW dipping fault system with displacement of ca. 150 ms (ca. 160 m) at the base of the Paleocene (Fig. 7). This fault terminates upwards within the Oligocene interval. Furthermore, an increasing thickness in the Eocene unit is shown, suggesting the faults were active during Eocene – Oligocene. Folded structures are also locally observed in the middle–upper Eocene strata (Fig. 6). Towards the south, Fault 3 appears to link with the faults of the eastern flank of the marginal high and marks the dramatic decrease of the Sub-basin B width.

5.1.3. Sub-basin C

Sub-basin C is bounded to the east by Fault 4 that is composed of segmented NW dipping faults that separate the sub-basin from the Veslemøy High (Fig. 1c). This fault shows a displacement of about 150 ms (ca. 160 m) at the base of the Paleocene and about 200 ms (ca. 210 m) at the base of lower Eocene seismic horizon (Fig. 5). An increasing thickness of the middle–upper Eocene strata in Sub-basin C suggests that there was a significant growth of the fault during this period. However, the observed Eocene growth across Fault 4 may be apparent, as the middle-upper Eocene strata may have been severely truncated below the base of the Pleistocene (Fig. 5). Sub-basin C comprises a similar tectonic style as seen for Sub-basin B. The minor faults primarily penetrate the Eocene interval suggesting that movement along these faults was responsible for part of Sørvestsnaget subsidence during the Eocene.

To the southwest, the faults seem to merge with the salt-influenced fault system that marks the transition to Sub-basin D (Fig. 6). A series of local mini-basins around the salt diapirs with Paleocene–Eocene sediment infilling and tilting of those strata towards the salt wall indicates active salt movement during early Cenozoic (Fig 7).

5.1.4. Sub-basin D

Sub-basin D is defined as the southernmost segment of the Sørvestsnaget Basin. It is bounded by Fault 4 to the north and Fault 5 that marks the transition to the Senja Ridge to the east (Fig. 1c). Fault 5 is a westerly dipping fault that terminates upwards within the Neogene strata. There is a high displacement (>750 ms) (ca. >785 m) of this fault at the base lower Eocene seismic horizon (Fig. 7). Another segment of this fault shows a major thickness increase in the middle–upper Eocene indicating significant fault growth. It is worth noting that the actual growth across the Fault 5 may be smaller as the Eocene might have been thicker on the Senja Ridge (Fig. 7)

Sub-basin D shows a thinning of Paleogene strata and the absence of the overlying Oligocene–Neogene unit (Fig. 6). Folded structures can be observed in this sub-basin (Fig. 6). To the west, the marginal high defines the western limit of the sub-basin (Fig. 8). Sub-basin D shows highly faulted lower Cenozoic strata with small displacements (<100 ms) (ca. <105 m) (Fig. 8). There is no clear structural delineation that separates this sub-basin from the Harstad Basin. However, a general thinning and onlap of the Oligocene–Neogene unit to the northwest likely marks the transition to the Harstad Basin (Fig. 6).

5.2. Oceanic basin sink: Lofoten Basin morphology

The Lofoten Basin is located to the west of Sub-basins A – D (Fig. 1c). This large oceanic deep-sea basin is bordered by the Mohns and Knipovich spreading ridges to the north, the Jan Mayen Fracture Zone and the Vøring Plateau to the west and the mainland Norway to the south (Fig. 1). The Senja Fracture Zone separates the Sørvestsnaget and Lofoten Basins and this zone marks the transition from the continental to oceanic crust (Faleide et al., 2008). The oceanic crust of the Lofoten Basin defines the base of the Cenozoic sediments.

The formation of oceanic crust west of the Senja Fracture Zone was initiated in the earliest Eocene and developed as a response to the rifting and sea-floor spreading between Norway and Greenland. Therefore, the Lofoten Basin shows a gradually younger infilling trend to the north (Fig. 13). The top of the oceanic crust is represented by a prominent acoustic impedance contrast in the seismic records and shows a reflection-free internal seismic character (Fig. 11). The oceanic crust shows an irregular topography with traces of extensional faulting. This rough morphology includes a series of peaks/ridges and troughs with heights reaching up to 750 ms (ca. 787 m). This extends for hundreds of kilometers with a general trend of increasing depth away from the mid-oceanic ridge.

5.3. Lower – middle Cenozoic lithology and seismic stratigraphy

Six key horizons, here named base Paleocene, base lower Eocene, base middle Eocene, base Oligocene, base Neogene, and base glacigenic sediments (R7 of Faleide et al., 1996) were mapped and tied with welltops from 7 boreholes across the study area. From these, the lower to middle Cenozoic succession has been subdivided into 5 major seismic units; Paleocene, lower Eocene, middle–upper Eocene, Oligocene, and Neogene as presented below.

5.3.1. Paleocene unit

Lithology: In Sub-basin C, well 7216/11-1S was terminated at 4215 m MSL (total depth - TD) in upper Paleocene (Danian) strata (Ryseth et al., 2003). In well 7216/11-1S, Paleocene strata are dominated by mudstone with occasional lenses of silty to very fine-grained sandstone at the bottom and an intercalation of limestone and dolomite stringers towards the top (Ryseth et al., 2003). They also reported the occurrence of diatoms and radiolarian. Knutsen et al. (1992) and Eidvin et al. (1993) described a similar lithology for Paleocene unit of wells 7119/7-1, 7117/9-1, and 7117/9-2.

Seismic expression: A higher amplitude reflection slightly below TD (ca. 3.75 s TWT) at well 7216/11-1S is assumed to represent the Mesozoic – Cenozoic boundary (Fig. 7). Paleocene strata are observed resting unconformably on deposits interpreted as Upper Cretaceous. In well 7016/2-1, the Paleocene unit is relatively thick (Fig. 8). Further east, the Mesozoic to Cenozoic transition is mapped with confidence in the area of the Veslemøy High and the Senja Ridge, where it was penetrated by wells 7117/9-1 and 7117/9-2 (Figs. 5 and 7). To the north, the deepest section that was penetrated by well 7316/5-1 is of late Paleocene age and the base Paleocene reflection is here interpreted to be located immediately below TD (Fig. 5). The Paleocene succession comprises low to high amplitude and sub-parallel seismic reflections across the study area (Figs. 5–7). In the area of Sub-basins B and C, the unit is slightly thinning towards the marginal high and the salt diapirs (Fig. 7). To the south, towards the Harstad Basin, mapping of Paleocene succession is hampered by the low seismic quality and resolution. A notable sediment thickness increase is observed in Sub-basin B and C towards the Bjørnøya Basin (Fig. 12a).

Paleoenvironment: In Tromsø Basin, a trace of low angle sediment progradation is observed from the Loppa High, suggesting that this High acted as source area for the Paleocene deposits of the Tromsø Basin (Fig. 5). In the Hammerfest Basin, there are no identifiable clinoforms from the Loppa High in the earlier stage of the Paleocene succession. However, the later stage shows a set of progradation from the Loppa High (Fig. 9). The increasing thickness towards the Bjørnøya Basin is interpreted to be due to sediment input from the northeast during this period. The generally uniform thickness of mud-dominated Paleocene interval indicates that these sediments were deposited during a tectonically quiet period dominated by deep marine hemipelagic sedimentation.

5.3.2. Lower Eocene unit

Lithology: In well 7117/9-2, only a thin layer of the uppermost Paleocene–lowermost lower Eocene deposits was described by Eidvin et al. (2000) (Fig. 7). In well 7216/11-1S of the Sørvestsnaget Basin, Ryseth et al. (2003) reported that the lower Eocene (Ypersian) is 180 m thick and consists of dark grey, laminated mudrock with abundant diatoms and radiolaria. This unit appeared thin in the Harstad Basin as shown from well 7016/2-1 (Fig. 8). In well 7316/5-1 in the Vestbakken volcanic province, volcanic deposit related to early Cenozoic volcanism occurred (Faleide et al., 1988).

Seismic expression: From seismic data, the lower Eocene unit conformably overlies the Paleocene unit and shows low to medium amplitude reflections with semi-parallel seismic internal reflections in most of the study area (Figs. 5–7). In the Vestbakken volcanic province to the north, there are abundant high amplitude and discontinuous reflection packages in the lower Eocene unit that are interpreted as volcanic deposits.

Paleoenvironment: The lower Eocene unit has a more limited areal extent towards the east compared to the underlying Paleocene unit (Fig. 12b). This unit is observed to be significantly thinning and eroded above the Senja Ridge (i.e. Fault 5) (Fig. 7). However, the growth of Fault 5 may be smaller due to erosion below the Pleistocene (Fig. 7). At the Veslemøy High, the lower Eocene unit is thicker and partly eroded and overlain by the base of the glacigenic sediments (Fig. 5). In contrast, the marginal high shows a thickening of the lower Eocene unit towards the flank of the high (Fig. 10b). The lower Eocene unit shows only a minor increase in thickness further south (Fig. 8). Although no major sediment progradation is observed, the lower Eocene unit displays a thickening of up to 2 km within the eastern part of Sub-basins B and C. Overall a deep marine environment is suggested based on well and seismic data.

5.3.3. Middle – upper Eocene unit

Lithology: Middle–upper Eocene was reported to be 722 m thick in well 7216/11-1S (Ryseth et al., 2003). In well 7316/5-1, middle Eocene strata are documented as predominantly shale with intercalated sandy packages by Eidvin et al. (1998). However, from their biostratigraphical study they reported that upper Eocene sediments were not present in this area. To the south, well 7016/2-1 shows thin strata which are inferred to be middle Eocene deposits (Fig. 8). In well 7117/9-2 on the Senja Ridge, the middle – upper Eocene section is missing (Eidvin et al., 2000).

Seismic expression: Seismic data show that, where present, the middle–upper Eocene unit rests conformably on the lower Eocene strata (Figs. 5–7). This seismic unit has low to high amplitude and relatively continuous, semi-parallel reflections in the Sørvesnaget Basin (Figs. 5–7). In the Vestbakken volcanic province to the north, this unit shows higher amplitude reflections in the upper succession (Figs. 5 and 11). The internal seismic signature also includes intervals with a clinoformal geometry, particularly in the Sørvestsnaget Basin.

Our seismic correlation shows that the middle–upper Eocene interval is not present or severely eroded on the Veslemøy High (Fig. 5). However, this unit shows apparent onlap onto the Veslemøy High. Onlap onto the salt diapirs is observed in the Sørvestnaget and Tromsø Basins. Towards the Lofoten Basin, this seismic unit thins and onlaps onto the oceanic crust (Figs. 11 and 13a).

A thinning of the middle–upper Eocene unit is observed westwards towards the marginal high, the intrabasinal high, and the basin margin (Fig. 12c). Truncation of middle–upper Eocene strata indicates an erosional surface (Fig. 10a). In the Vestbakken volcanic province, this unit shows an increased thickness up to 3,500 m, indicating that this area was a main depocenter.

Paleoenvironment: The supply of sediments during the middle to late Eocene formed sandy deep-water fans and are inferred to have been sourced from the Stappen High (Safronova et al., 2012). The N–S trending clinoforms are present mostly within Sub-basins B and C, with a possible extension into Sub-basin D (Fig. 6). However, results from well 7016/2-1 show no identifiable middle Eocene sand suggesting a limitation of this deep-marine sandy system towards the Harstad Basin. A similar clinoform pattern is also observed in the Tromsø Basin and most likely sourced from the Loppa High (Knutsen et al., 1992). In addition, significant thickness of middle–upper Eocene sediments across the Sørvestsnaget Basin suggests a regional basin deepening/major subsidence (Figs. 5–7). The available data show that overall a deep marine environment prevailed with significant clastic input from the major structural highs.

5.3.4. Oligocene unit

Lithology: In well 7316/5-1 in the Vestbakken volcanic province, Oligocene deposits are represented by marine shales deposited above a major stratigraphic break (Eidvin et al., 2014). In well 7216/11-1S in the Sørvestsnaget Basin, the Oligocene interval is comprised primarily of mudstones that were interpreted to be deposited in a shallow marine environment (Ryseth et al., 2003). Well 7016/2-1 shows that Oligocene deposits also present in the Harstad Basin (Fig. 8). Biostratigraphical analysis from well 7117/9-1 and 7117/9-2 on the Senja Ridge shows no identifiable Oligocene deposits (Eidvin et al., 1993).

Seismic expression: The Oligocene unit is dominated by low to medium amplitude and relatively continuous seismic reflections (Figs. 5–7). The contact with the underlying Eocene seismic unit is conformable, although, in the area of the intrabasinal high the contact appears to be irregular suggesting an unconformity (Fig. 5). To the east, the Oligocene unit is observed to be truncated by the base of the glacigenic sediments (Figs. 6 and 7). To the west, onlap of the seismic unit towards the marginal high is observed (Figs. 8 and 10). These onlaps suggest that the marginal high was a bathymetric high during the Oligocene (e.g. Ryseth et al. 2003). Based on similarities in seismic reflection patterns, the unit is interpreted to continue west of the marginal high and into the Lofoten Basin (Fig. 13b).

Paleoenvironment: An overall shallow marine environment is suggested by Ryseth et al. (2003) from well and biostratigraphy analysis. Our seismic mapping shows a thinner Oligocene succession in the eastern part of the marginal high compared to the western part (Fig. 10b). The marginal high might have restricted sediment input into the Lofoten Basin. The Oligocene deposits may have been routed into the Lofoten Basin by gravity flows. The marginal high itself may also have been eroded shedding sediment to the west. The Senja Ridge may have acted as a paleohigh since no Oligocene sediments are observed or Oligocene deposits were later eroded. A notable thickening of Oligocene sediments is also observed in Sub-basin C where it has a maximum thickness of 1750 m (Fig. 12d). The sediment infill of Sub-basin A may have also been sourced locally from the intrabasinal high (Fig 6). Sediment thickening towards the high may have been caused by the creation of accommodation space through fault reactivation as well as relative uplift (and erosion) of the intrabasinal high during the earliest Oligocene times (Figs. 5 and 9).

5.3.5. Neogene unit

Lithology: In well 7216/11-1S in the Sørvestsnaget Basin, a 100 m thick Miocene shallow-marine, muddy succession was encountered starting at a depth of 2246 m MSL (Ryseth et al., 2003). This unit is present in well 7316/5-1 in Vestbakken volcanic province but not identifiable in well 7016/2-1 in the Harstad Basin despite seismic mapping showing a continuation of the Neogene unit adjacent to this well (Fig. 8).

Seismic expression: The Neogene unit shows low to medium amplitude reflections and has a parallel internal reflection geometry (Figs. 5–7). It is also observed to onlap the marginal high and it has a conformable contact with the underlying Oligocene unit. The overlying glacigenic sediments rest unconformably on the top of the Neogene unit. This unit has a more limited distribution compared to the underlying Oligocene unit (Fig. 12e). Sub-basin A comprises the thickest of the Neogene deposits with a maximum thickness of 917 m, particularly in the area just south of the Vestbakken volcanic province (Figs. 6 and 12). Here, the Neogene unit shows an acoustically parallel signature with a climbing mound geometry and is interpreted as contourites (Figs. 7 and 10). Within Sub-basin B, this unit is truncated by the glacigenic wedge to the east towards the Senja Ridge and the Veslemøy High (Figs. 5 and 7). In addition, a major sediment accumulation is observed in the Lofoten Basin to the west (Figs. 11 and 13c).

Paleoenvironment: Well data show that the Neogene period in the study area was dominated by relatively a shallow marine environment. Seismic data from the slope area to the west suggest contourites, implying a slope to deeper marine environment (Fig. 10b).

5.4. Early – middle Cenozoic erosion, erosion rates and sediment yield

The Sørvestsnaget Basin and Lofoten Basin along with the adjacent basins were key depocenters during the Paleogene–Neogene period as shown from the sub-basins infilling and stratigraphy (Figs. 12f and 13d). Our sediment volume estimations were obtained by summing up the volume within the eastern part (southwestern Barents Sea basins and highs) and the western part (the Lofoten Basin) of the study area (see Fig. 4), which correspond to 296,500 km^3. From this, the total corrected sediment volume for the Paleogene–Neogene in the southwestern Barents Sea and Lofoten Basin is about 280,200 km^3 (Table 1). This number is used to calculate the sedimentation rate (Table 2). There are a number of uncertainties for the sediment volume calculation that are addressed below.

a) Sink (10^3 km^3)

Initial total volume from isopachs		296,5
Corrections	Volume correction of (i) ooze sediments for Paleocene, Eocene, Oligocene units and (ii) contouritic sediment for Neogene unit (substract 10% of the deposits)	266,8
	Volume correction due to decompaction (add 5%)	280,2
Corrected total volume of sediment that has been deposited from the considered source area		280,2

b) Source (10^3 km^3)

Corrected total volume of the sink area = eroded from source area		280,2
Corrections	Volume correction due to bedrock composition of the source area (substract 10% of the deposits)	252,1
Corrected total volume of the source area		252,1

Table 1. Volume correction for the (a) sink deposits as isopached and (b) the inferred volume as eroded from the source area.

5.4.1. Volume correction due to the processes of deposition

Within the Paleogene succession, some biogenic ooze (silica) was present in well 7216/11-1S (Ryseth et al., 2003). Further north, well 7316/5-1 also shows biogenic ooze sediments at this interval (Eidvin et al., 1998). As these sediments were derived from biogenic production of the Paleocene ocean (within the basins) and not from erosion of the Barents Sea shelf, they should not be included in the total volume of erosional products. Though, it is difficult to quantify the volume of ooze in this interval based on the data available. The total sediment volume has tentatively been reduced by 10% to account for these deposits.

As part of the Neogene sediments, contourites were also not derived from the Barents Sea shelf but were deposited by ocean currents most likely from south of the study area (Laberg et al. 2005). Therefore, Neogene sediment volume has been reduced by 10% to compensate for this deposit (Lasabuda et al., 2018). The total volume for the lower to middle Cenozoic succession is 266,800 km^3 after the corrections have been applied. From this, the following correction will be applied (Table 1).

5.4.2. Volume correction due to the overburden compaction

Lower to middle Cenozoic units are presently buried under the thick glacigenic sediment wedge, that results in the compaction of the deposits. To compensate for this overburden, the volume of sediments (266,800 km^3) will be adjusted using an average decompaction correction of 5 % (Table 2). As an example, fine grain Eocene sandstone in well 7216/11-1S with present depth of ca. 3 km (Ryseth et al., 2003) will be compacted ca. 5% according to the diagram of vertical effective stress relation with porosity (Bjørlykke and Høeg, 1997; Bjørlykke et al., 2015). The applied decompaction correction results in a total sediment volume of about 280,200 km^3 (Table 1). This volume is then used to calculate the sedimentation rate (Table 2).

Periods considered (Ma)	Sediment volume (10^3 km^3)	Depositional area (10^3 km^2)	Sedimentation rates (m/k.y)
Neogene (23.03 – 2.58)	96	171.6	0.027
Oligocene (33.9 – 23.03)	45.3	130.9	0.032
Eocene (56 – 33.9)	99.6	119.6	0.038
Paleocene (66 – 56)	39.3	55.7	0.071
Paleogene–Neogene (66 – 2.58)	280.2	171.6	0.026

Table 2. Sediment volume, depositional area and sedimentation rates for the early to middle Cenozoic period. The chronology is according to Cohen et al. (2016).

5.4.3. Volume correction due to the bedrock composition of the source area

To quantify the total erosion of the source area and the corresponding erosion rates, we have to relate the volume of the sediment deposited to their source area. In this study, we assume that the volume of the deposited sediments was higher than the volume of eroded rocks in the source area. This is because up to half of our drainage area is located within mainland Norway which consists of more compacted crystalline rocks. The remainder is interpreted to be derived from sedimentary rocks on the shelf. In a study of the glacial erosion of the crystalline bedrock of mid-Norway, Dowdeswell et al. (2010) suggested a correction for the bedrock compaction of 20% for sediments sourced from crystalline bedrock. This is due to density differences between sedimentary rock (2.2 gr/cm^3 from Table 3) and the crystalline rock (ca. 2.7 gr/cm^3). Following this and our estimation that half of our source area to comprise crystalline rocks, our bedrock volume has been corrected by subtracting the total volume of sediment deposited (280,200 km^3) with a compaction volume of 10% resulting in a value of about 252,100 km^3 (Table 1). No correction was applied for the source area composed from sedimentary rocks.

5.4.4. Total sediment volumes and depositional areas

The total volume of Paleogene–Neogene sediment that has been deposited from the source area are estimated to be about 280,200 km^3. This number is higher than the results from Fiedler and Faleide (1996) and Vorren et al. (1991), which reported values of 162,000 km^3 and 206,500 km^3, respectively. These variations are likely due to a more detailed interpretation of the depositional area from an expanded database.

The maximum total depositional area for Paleogene–Neogene sediments is about 171,600 km^2. Throughout the period considered, there is a systematic increase in the depositional area from the Paleocene to the Neogene, covering 55,700 km^2 and 171,600 km^2, respectively (Table 2). This increase of the depositional area is due to the relative northward progressive sea-floor spreading within the Norwegian – Greenland Sea.

5.4.5. Sedimentation rates

The average sedimentation rate for the Cenozoic's pre-glacial period is 0.026 m/k.y. and shows a gradual decrease from 0.071 m/k.y during the Paleocene to 0.027 m/k.y in the Neogene. (Table 2). The numbers presented here are regarded as minimum estimates due to the later uplift and erosion during late Cenozoic period that led to erosion and removal of part of these deposits.

5.4.6. Sediment yield

The sediment yield for the pre-glacial period shows an average value of 26.2–45.7 t/km^2/y (Table 4). The sediment yield was derived by dividing the sediment discharge by the size of the drainage basin (Table 4). When calculating this value, the average sediment density was derived from well-logs data (Table 3). There are two estimated sizes of the source area during this period, 191,500 and 334,000 km^2, which is about 33% smaller and 16% larger compared to Fiedler and Faleide (1996), respectively. These two alternatives are regarded as minimum and maximum estimates. The source areas were delineated according to the paleogeography and paleoenvironmental reconstruction for each period as will be further discussed below.

Periods considered (Ma)	Well (gr/cm^3)						All wells (gr/cm^3)
	7216/11-1S	7117/9-1	7117/9-2	7316/5-1	7119/7-1	7218/8-1	
Neogene (23.03 – 2.58)	2.24	-	-	2.15	-	-	2.2
Oligocene (33.9 – 23.03)	2.31	-	-	2.12	-	-	2.22
Eocene (56 – 33.9)	2.37	1.96	-	2.39	2.01	-	2.18
Paleocene (66 – 56)	2.36	1.97	1.86	2.49	2.23	2.24	2.19
					Paleogene–Neogene		2.2

Table 3. Sediment density (gr/cm^3) derived from well logs for each period.

5.4.7. Net erosion and erosion rates of the source area

Average pre-glacial net erosion is calculated from the size of the drainage basin and sediment yield in accordance with Vorren et al. (1991), which yields total average erosion values of 858 m (for maximum source area) or 1362 m (for minimum source area). The erosion estimates are observed to be highest in the Eocene and Neogene periods, reaching values of 325–487 m and 259–469 m, respectively. In addition, the average erosion rates for the Paleogene–Neogene are estimated to be 0.014–0.021 m/k.y and show almost the same value throughout the pre-glacial period (Table 4).

Periods considered (Ma)	Volume of the source area (10^3 km^3)	Sediment discharge (10^6 t/y)*	Drainage area (10^3 km^2)		Sediment yield (t/km^2/y)		Erosion (m)		Erosion rates (m/k.y.)	
			Min	Max	Min	Max	Min	Max	Min	Max
Neogene (23.03 – 2.58)	86.4	9.3	184.1	334	27.8	50.5	259	469	0.013	0.023
Oligocene (33.9 – 23.03)	40.8	8.3	184.1	334	24.9	45.3	122	222	0.011	0.02
Eocene (56 – 33.9)	89.6	8.8	184.1	275.8	32.1	48	325	487	0.015	0.022
Paleocene (66 – 56)	35.4	7.7	191.5	232.6	33.3	40.4	152	185	0.015	0.018
Paleogene–Neogene (66 – 2.58)	252.1	8.7	191.5	334	26.2	45.7	858	1362	0.014	0.021

*sediment density from Table 3

Table 4. Bedrock volume, sediment discharge, drainage basin area, sediment yield, and erosion estimated for the southwestern Barents Sea for the pre-glacial periods within the Cenozoic.

5.4.8. Other uncertainties in the presented approach and their constraints

Beside the corrections and assumptions that are mentioned above, our estimations include an uncertainty in the time-to-depth conversion and seismic data distribution. A more precise seismic velocity analysis would have improved the depth conversion. A better seismic data coverage and more well data in the oceanic sink (Lofoten Basin) would have resulted in a more precise estimate of the sediment volume deposited and corresponding age control (Fig. 11). In addition, volcanics are a significant component of the lower Eocene in the Vestbakken volcanic province. However, in a regional context, these deposits are considered less likely to reach a volume that influence the total sedimentary budget for the Eocene succession.

6. Discussion

6.1. Early – middle Cenozoic tectonosedimentary development of the western margin and average sedimentation rates

The southwestern Barents Sea continental margin has undergone various phases of tectonism since the early Cenozoic, that have controlled the spatial distribution and temporal evolution of the source area erosion and the corresponding sedimentary environment of the depositional area. The southern study area (Sub-basins C, D and the Harstad Basin) has experienced transtension in a relatively narrow zone between the marginal high and the Senja Ridge. Conversely, the northern part of the Sørvestsnaget Basin (Sub-basin A, B) experienced a gradual change from transtension to extension in the Vestbakken volcanic province (Figs. 14a and b). To the north, the Stappen High and part of the Bjørnøya Basin was uplifted, accommodated by the Knølegga Fault Complex, probably due to footwall uplift associated with the breakup (e.g. Sættem et al., 1994; Blaich et al., 2017).

The sediment depocenter during the Paleocene–early Eocene was located in the northern part of the Sørvestsnaget Basin, southwest of the Bjørnøya Basin (Figs. 12a and b). The Paleocene sediments were deposited at an average sedimentation rate of 0.071 m/k.y. The southern part of the Sørvestsnaget Basin comprises thinner Paleocene–lower Eocene deposits, likely related to thermal effects of the early seafloor opening that caused uplift of the basin floor. The uplift of the marginal high was initiated during the earliest Eocene and related to the shear margin development. The sediment distribution suggests that the intrabasinal high and Veslemøya High remained part of the basin depocenter in the Paleocene–early Eocene (Figs. 12a, b).

The earlier stage of the Paleocene succession show that the Loppa High might have been part of the broad Paleocene depocenter as also suggested by Prøis (2015). However, later in the Paleocene, the Loppa High might have formed a positive feature supplying sediment to the Hammerfest Basin and the Tromsø Basin (e.g. Knutsen and Vorren, 1991) (Fig. 9).

The pronounced middle–late Eocene subsidence of the Sørvestsnaget Basin resulted in the accumulation of a large volume of sediment from the uplifted Stappen High (Fig. 14c). The deep-marine setting persisted into the middle–late Eocene period with differential subsidence of the sub-basins. Major subsidence is also observed in the Tromsø Basin receiving sediment from the Loppa High (Knutsen et al., 1992). An average sedimentation rate of 0.038 m/k.y has been estimated for the Eocene period. The Veslemøya High was established as a positive feature and it may have acted as a source for some of the sediments deposited in the adjacent basins (Fig. 5). The salt may have been active in this period (Knutsen and Larsen, 1997). There is a major shift of sediment accumulation from Sørvestsnaget Basin, during Paleocene–early Eocene, to Vestbakken volcanic province, during the middle–late Eocene, which was accommodated by the contemporaneous fault growth.

The major plate reorganization during the earliest Oligocene likely resulted in renewed uplift and erosion of the Stappen High and the formation of the intrabasinal high. A stratigraphic break at the upper Eocene–Oligocene boundary at well 7216/11-1S may also be related to uplift and erosion (Ryseth et al., 2003). The sparse but similar results of the well data suggest that the middle Cenozoic uplift was widespread but was perhaps not as strong as in the early Cenozoic. Lack of seismic signature showing fold or shortened structures in the Oligocene strata indicate that the uplift was likely related to crustal thinning or rift-flank uplift processes. This mechanism can be explained as a result of the Greenland plate moving together with the north American plate, after which the western Barents Sea continental margin experienced NW extension and sea-floor opening (Eldholm et al., 1987).

The intrabasinal high is inferred to have been formed during the Eocene–Oligocene transition while the marginal high became largely stationary (Fig. 14d). Although the contraction structures found in the central and southern part of Sørvestsnaget Basin are interpreted to be formed at the same time (Kristensen et al., 2017), this relative uplift in the northern Sørvestsnaget Basin was likely due to thermal effects (e.g. Blaich et al., 2017) creating heat transfer contemporaneous with the progressive sea-floor spreading. The weakening due to the formation of hyperextended crust along the northeastern Atlantic margin is expected to have reached the southwestern Barents Sea area contributing to uplift of such features (Lundin and Doré, 2011). Oligocene sediments were likely sourced from the east and were deposited at a minimum average rate of 0.032 m/k.y.

The paleoslope morphology west of the marginal high and Vestbakken volcanic province suggests deposition of contouritic sediment, indicating that the southwestern Barents Sea slope from this time onward was affected by alongslope ocean currents (Figs. 14e and 15d). These currents most likely were part of the general circulation of the Norwegian – Greenland Sea (Laberg et al., 2005). Average sedimentation rates for the Neogene period are approximately 0.027 m/k.y. The establishment of the ocean circulation system at this time may be related to the opening of the Fram Strait as discussed by Kristoffersen (1990) and Engen et al. (2008). The Neogene succession is capped by an erosional truncation surface. This is due to the late Cenozoic glacial erosion that affected the southwestern Barents Sea (Fig. 14f).

6.2. Early – middle Cenozoic erosion affecting the southwestern Barents Sea shelf

Here, the quantification of early to middle Cenozoic erosion in the inferred source area will be discussed based on plate reconstruction using the GPlates software v. 2.0 (Matthews et al., 2016; Müller et al., 2016) and paleoenvironmental reconstruction (Fig. 15). The erosion estimates are compared to previous work including studies quantifying the erosion in the glacial period as well as present-day fluvial and coastal systems.

6.2.1. Early – middle Cenozoic source area and erosion estimates

The estimated net erosion varies from approximately 858 to 1362 m affecting an area of 191,500–334,000 km^2 of the Barents Sea during the early to middle Cenozoic. The main uncertainty relates to the eastern limit of the sediment source area. The maximum estimate also includes part of the present continental shelf, east of the Loppa High. The erosion is inferred to mainly have affected the highs and ridges. Paleogene clinoforms in the basins west and south of the Stappen High and Loppa High support this interpretation (Figs. 5 and 9). The mainland of Northern Norway is also considered as a key area subjected to erosion during early to middle Cenozoic period although so far, only few details are known (Vorren et al., 1991).

At the end of Paleocene, the drainage area for the southwestern Barents Sea is interpreted to have included the Stappen High, the Loppa High, part of Bjarmeland Platform and mainland Northern Norway covering an area of up to 232,600 km^2 (Fig. 15a). We estimated the net average Paleocene erosion of the source area to correspond to 152–185 m of erosion. There was likely a very low sediment input from mainland Greenland to the Lofoten Basin due to the structural configuration of the NE Greenland shelf. Some sediments were trapped in the Danmarkshavn Basin, in the Danmarkshavn Ridge area, and the Thetis Basin (Petersen et al., 2015). The development of a marginal high at the shelf edge may have acted as an additional sediment barrier preventing input to the Lofoten Basin (Tsikalas et al., 2005; Petersen et al., 2015)

During the early phase of rifting between Norway and Greenland, unstable sediments on the flank of the emerging ocean basin may have contributed directly to the Lofoten Basin infilling through gravity driven processes. To the north, Svalbard was uplifted during early Cenozoic that led to the development of the West Spitsbergen Fold-Thrust Belt supplying sediment predominantly to the east. Studies from the Central Basin of Svalbard show a shallow-marine dominated succession, implying that the southern Barents Sea shelf may have been below sea-level at the end of Paleocene (Helland-Hansen, 2010).

Towards the end of the Eocene, the estimated source area likely incorporated a wider area to the east (the Finnmark and Bjarmeland Platforms), as well as part of Gardarbanken and Sentralbanken high (Fig. 15b). Here, the drainage area corresponds to an area of 275,800 km^2, as the wider Barents Sea area has been interpreted to have been uplifted and subjected to erosion (Smelror et al., 2009). The contemporaneous development of the deep Lofoten Basin to the west probably regressed the Barents Sea shelf and exposed the area to erosion. The Greenland-Norwegian transpression may have affected the area between Svalbard and the Stappen High, leading to the formation of this area as a positive feature (Lasabuda et al., 2018). This region could then have acted as a source area for some of the sediments deposited in the southwestern Barents Sea area. Alternatively, our conservative (minimum) delineation of the drainage area implies that the Stappen and Loppa Highs as well as mainland Norway remained the core areas (184,100 km^2). From this, the total average erosion during the Eocene was between 325 m (at the maximum source area) and 487 m (at the minimum source area).

During the Oligocene, the estimated source area still corresponded to approximately 184,100 to 334,000 km^2. We calculated that an average 122–222 m of sediment was removed due to erosion. The combination of a non-marine and coastal plain setting has been a favored interpretation for a large area in the southwestern Barents Sea (Smelror et al. 2009) (Fig. 15c). Besides the Finmark and Bjarmeland Platforms, the drainage area may have extended up to the

Gardarbanken and Sentralbanken high. In addition, we consider the Edgeøya platform as the area supplying sediment to the northwestern margin of the Barents Sea (Hjelstuen et al., 1996; Lasabuda et al., 2018), which is outside our study area (Fig. 15c).

The source area for the Neogene period is considered as a continuation of the late Oligocene setting implying no significant change to the drainage area (Fig. 15d). The average net erosion is estimated to be 259–469 m. Two identified stratigraphic breaks from well 7216/11-1S are documented at the Oligocene–Miocene boundary and middle–upper Miocene boundary, respectively (Ryseth et al., 2003), which are in conformity with this interpretation. Shallow core analysis shows a lower Oligocene–lower Miocene hiatus at the Vestbakken volcanic province (Sættem et al., 1994). These breaks could be related, at least partly, to ocean current erosion following the establishment of the present-day pattern of circulation during the Miocene (Haq et al., 1987; Rydningen et al., in prep.).

6.2.2. How do our results (the rates) compare to previous studies?

Our estimated average sedimentation rate of 0.026 m/k.y. for the early to middle Cenozoic periods is at the same order of magnitude as the rates reported from previous studies from this area. Vorren et al. (1991) and Fiedler and Faleide (1996) found a value of 0.031 m/k.y. and 0.022 m/k.y., respectively. For the NE Greenland, a similar order of magnitude of average sedimentation rate (0.036 to 0.02 m/k.y.) for the last 51 to 15 m.y. has been reported (Berger and Jokat, 2008). Our average erosion rates have been estimated to be 0.014–0.021 m/k.y. for the early to middle Cenozoic periods. This is also in agreement with the average rate of 0.012 m/k.y from Fiedler and Faleide (1996).

For the succeeding glacial period, similar studies done in the southwestern Barents Sea by Laberg et al. (2012) and offshore mid-Norway by Dowdeswell et al. (2010) reported averaged sedimentation rates of 0.28–0.36 m/k.y and 0.24 m/k.y, respectively. Laberg et al. (2012) also estimated an average erosion rate of 0.4 m/k.y for the glacial period. Thus, the average sedimentation and erosion rates presented in this work are one order of magnitude lower compared to the rates reported for the succeeding glacial period. These findings testify to the effectiveness of the ice in eroding the source area and the amplification of glacial isostatic uplift.

6.2.3. Early – middle Cenozoic net erosion of the southwestern Barents Sea shelf

Our estimated average net erosion for early – middle Cenozoic is 858 to 1362 m. Fiedler and Faleide (1996) documented an average net erosion of only about 562 m. In a more recent study, Baig et al. (2016) estimated total net Cenozoic erosion reached values of 1700 m and 2100 m for Bjørnøya trough areas and the Stappen High, respectively. By subtracting the late Cenozoic erosion estimated by Laberg et al. (2012), this implies a pre-glacial net erosion values of 600–700 m in the trough area and 1450–1600 m for the Stappen High (Baig et al., 2016). These numbers are in agreement with our average net erosion.

A recent study using apatite (UeTh)/He thermochronology by Zattin at al. (2016) shows an average total Cenozoic net erosion of 1000 m in the area of the Bjørnøyrenna Fault Complex (immediately west of the Loppa High) and demonstrates a key phase of late Miocene–early Pliocene uplift. They documented a lack of an identifiable late Pliocene–Pleistocene uplift phase from glacial erosion. This may be due to the compensating effect of loading of the glacial erosional product (subsidence) to the west (the Bear Island TMF).

In conclusion, our result shows that the estimated pre-glacial net erosion mainly affected the highs of the Barents Sea shelf and mainland Northern Norway. The western margin was an area of sediment deposition. Finally, the pre-glacial erosion has a considerable contribution to the total Cenozoic net erosion in this area.

6.2.4. Early – middle Cenozoic sediment discharge

The highs and ridges of the source area can be interpreted as subaerial parts of a low-relief coastal or shallow-marine platform. Fluvial erosion and coastal erosion may have been important processes in the erosion of the highs and ridges. We tested this hypothesis by estimating the sediment discharge and compared it to those of present-day fluvial and coastal systems.

The estimated sediment discharge shows only minor variation for the whole early to middle Cenozoic with an average discharge of $8.7x10^6$ t/yr. There is also only a minor variation in sediment yield estimated for the Paleogene–Neogene ranging from 26.2–45.7 $t/km^2/yr$. Our estimated values are in conformity with the results reported for present-day fluvial system by Milliman and Meade (1983) and Sømme et al. (2009) (Fig. 16). The relation of our sediment yield and drainage basin area matches with the values reported from present-day low yield rivers in Africa and the Eurasian Arctic (Fig. 16a). Our results also conform reasonably well with the values reported from areas of tectonically active and passive systems (Fig. 16b).

Furthermore, our study shows estimated values comparable to those from studies of present-day coastal erosion from New Zealand (Gibb, 1978), the Canadian Beaufort Sea and Laptev Sea (Rachold et al., 2000). To conclude, our estimated sediment discharge and size of source area are considered likely estimates as they are relatively similar to those of present-day systems.

7. Conclusions

The main results of our study can be summarized as follows:

- During the transition from late Paleocene to early Eocene, the southwestern Barents Sea continental margin was affected by the initiation of the sea-floor spreading between Norway and Greenland. Tectonostratigraphic analysis of sub-basins within Sørvestsnaget Basin shows an overall transtensional setting. In the Paleocene, basin fill was mainly derived from the erosion of Stappen High, the Loppa High, and mainland Norway covering areas of 191,500–232,600 km^2. Little sediment from NE Greenland is inferred to have reached the studied basins. Throughout the Paleocene, an estimated 152–185 m of sediment was removed from the source areas at an average erosion rate of 0.015–0.018 m/k.y. In the basins, sediments were deposited at an average sedimentation rate of 0.071 m/k.y.
- The Eocene was a period of major tectonic uplift for most of the positive structural elements in the southwestern Barents Sea. The marginal high shows main growth during this time. This was also the period of subsidence and volcanism in the Vestbakken vocanic province. Throughout the Eocene, thick successions of deep-marine sediments were deposited including middle Eocene submarine fans in the Sørvestsnaget Basin sourced from the Stappen High. The Loppa High and mainland Norway have also acted as a prominent sediment source. The average sedimentation rate during the Eocene was 0.038 m/k.y. During this period, the source area of 184,100–275,800 km^2 experienced an average net erosion of 325–487 m at an erosion rate of 0.015–0.022 m/k.y.
- In the Oligocene, a period of relative uplift affected the northern part of the Sørvestsnaget Basin (intrabasinal high) with possible continuation to the Stappen High. The sediments were derived largely from the east with estimated source areas of 184,100–334,000 km^2. The sedimentation rate and erosion rate are 0.032 m/k.y. and 0.011–0.02 m/k.y., respectively. On average, between 122–222 m of sediment was eroded during the Oligocene period.

- The sedimentation pattern and the size of the source area in the Neogene is inferred to be similar as in the Oligocene. A shallow marine environment may still have prevailed during the Neogene. To the west, contouritic sediments developed at the newly formed eastern slope of the deep-marine Lofoten Basin suggesting influence of alongslope ocean currents. The average sedimentation rate during the Neogene is 0.027 m/k.y. The erosive event may be explained in association with global sea level fall or the contour current processes. The average net erosion in the Neogene is estimated to be 259–469 m with a rate of 0.013–0.023 m/k.y.
- The total average net erosion of the southwestern Barents Sea shelf for the early–middle Cenozoic is calculated to be 858–1362 m with an average rate of 0.014–0.021 m/k.y that affected an area of 191,500–334,000 km^2. The average sedimentation rate is 0.026 m/k.y which is markedly lower than the glacial period. The result of this study shows a variation in different structural elements in different periods and documents a significant pre-glacial erosion in part of the southwestern Barents Sea, thus provides the basis for more precise calculation of the maximum burial history for this area.

Acknowledgements

This paper was part of the Research Centre for Arctic Petroleum Exploration (ARCEx) project, which is funded by the Research Council of Norway (grant number 228107) and ARCEx partners. We thank TGS/Spectrum for the permission to publish the seismic profiles. Schlumberger is acknowledged for the software under the educational license agreement for Department of Geosciences, UiT – The Arctic University of Norway. Proofreading by Ryan Dillon and Laura Swinkels are highly appreciated. We are grateful to Jan Inge Faleide and Alf Ryseth for providing constructive comments on the manuscript. Alvar Braathen, Tom Arne Rydningen, and Sri Wulan Susilo are thanked for valuable discussions. Helpful reviews by Michael Elliot Smith and Editor Thomas Hadlari are much appreciated.

References

Anell, I., Thybo, H., Artemieva, I., 2009. Cenozoic uplift and subsidence in the North Atlantic region: Geological evidence revisited. Tectonophysics 474, 78-105.

Baig, I., Faleide, J.I., Jahren, J., Mondol, N.H., 2016. Cenozoic exhumation on the southwestern Barents Shelf: Estimates and uncertainties constrained from compaction and thermal maturity analyses. Mar. Pet. Geol. 73, 105-130.

Berger, D., Jokat, W., 2008. A seismic study along the East Greenland margin from 72 N to 77 N. Geophys. J. Int. 174, 733-748.

Bergh, S.G., Braathen, A., Andresen, A., 1997. Interaction of basement-involved and thin-skinned tectonism in the Tertiary fold-thrust belt of central Spitsbergen, Svalbard. AAPG Bull. 81, 637-661.

Bergh, S.G., Grogan, P., 2003. Tertiary structure of the Sorkapp-Hornsund region, south Spitsbergen, and implications for the offshore southern extension of the fold-thrust belt. Norsk Geol. Tidsskr. 83, 43-60.

Bjørlykke, K., Høeg, K., 1997. Effects of burial diagenesis on stresses, compaction and fluid flow in sedimentary basins. Mar. Pet. Geol. 14, 267-276.

Bjørlykke, K., Høeg, K., Mondol, N.H., 2015. Introduction to Geomechanics: stress and strain in sedimentary basins, Petroleum Geoscience. Springer, 301-318.

Blaich, O., Tsikalas, F., Faleide, J., 2017. New insights into the tectono-stratigraphic evolution of the southern Stappen High and its transition to Bjørnøya Basin, SW Barents Sea. Mar. Pet. Geol. 85, 89-105.

Braathen, A., Bergh, S., Maher, H., 1995. Structural outline of a Tertiary Basement-cored uplift/inversion structure in western Spitsbergen, Svalbard: Kinematics and controlling factors. Tectonics 14, 95-119.

Butt, F.A., Drange, H., Elverhøi, A., Otterå, O.H., Solheim, A., 2002. Modelling Late Cenozoic isostatic elevation changes in the Barents Sea and their implications for oceanic and climatic regimes: preliminary results. Quat. Sci. Rev. 21, 1643-1660.

Cavanagh, A.J., Di Primio, R., Scheck-Wenderoth, M., Horsfield, B., 2006. Severity and timing of Cenozoic exhumation in the southwestern Barents Sea. J. Geol. Soc. 163, 761-774.

Cohen, K., Finney, S., Gibbard, P., Fan, J.-X., 2016. The ICS international chronostratigraphic chart. Episodes 36, 199-204.

Dimakis, P., Braathen, B.I., Faleide, J.I., Elverhøi, A., Gudlaugsson, S.T., 1998. Cenozoic erosion and the preglacial uplift of the Svalbard–Barents Sea region. Tectonophysics 300, 311-327.

Doré, A., Cartwright, J., Stoker, M., Turner, J., White, N., 2002. Exhumation of the North Atlantic margin: introduction and background. Geol. Soc., London, Spec. Publ. 196, 1-12.

Doré, A., Jensen, L., 1996. The impact of late Cenozoic uplift and erosion on hydrocarbon exploration: offshore Norway and some other uplifted basins. Global Planet. Change 12, 415-436.

Dowdeswell, J.A., Ottesen, D., Rise, L., 2010. Rates of sediment delivery from the Fennoscandian Ice Sheet through an ice age. Geology 38, 3-6.

Eide, C.H., Klausen, T.G., Katkov, D., Suslova, A.A., Helland-Hansen, W., 2017. Linking an Early Triassic delta to antecedent topography: Source-to-sink study of the southwestern Barents Sea margin. Geol. Soc. Am. Bull. https://doi.org/10.1130/B31639.1

Eidvin, T., Goll, R.M., Grogan, P., Smelror, M., Ulleberg, K., 1998. The Pleistocene to Middle Eocene stratigraphy and geological evolution of the western Barents Sea continental margin at well site 7316/5-1 (Bjørnøya West area). Norsk Geol. Tidsskr. 78, 99-124.

Eidvin, T., Jansen, E., Riis, F., 1993. Chronology of Tertiary fan deposits off the western Barents Sea: implications for the uplift and erosion history of the Barents Shelf. Mar. Geol. 112, 109-131.

Eidvin, T., Jansen, E., Rundberg, Y., Brekke, H., Grogan, P., 2000. The upper Cainozoic of the Norwegian continental shelf correlated with the deep sea record of the Norwegian Sea and the North Atlantic. Mar. Pet. Geol. 17, 579-600.

Eidvin, T., Riis, F., Rasmussen, E.S., 2014. Oligocene to Lower Pliocene deposits of the Norwegian continental shelf, Norwegian Sea, Svalbard, Denmark and their relation to the uplift of Fennoscandia: A synthesis. Mar. Pet. Geol. 56, 184-221.

Eldholm, O., Faleide, J.I., Myhre, A.M., 1987. Continent-ocean transition at the western Barents Sea/Svalbard continental margin. Geology 15, 1118-1122.

Engen, Ø., Faleide, J.I., Dyreng, T.K., 2008. Opening of the Fram Strait gateway: A review of plate tectonic constraints. Tectonophysics 450, 51-69.

Faleide, J., Myhre, A., Eldholm, O., 1988. Early Tertiary volcanism at the western Barents Sea margin. Geol. Soc., London, Spec. Publ. 39, 135-146.

Faleide, J.I., Solheim, A., Fiedler, A., Hjelstuen, B.O., Andersen, E.S., Vanneste, K., 1996. Late Cenozoic evolution of the western Barents Sea-Svalbard continental margin. Global Planet. Change 12, 53-74.

Faleide, J.I., Tsikalas, F., Breivik, A.J., Mjelde, R., Ritzmann, O., Engen, O., Wilson, J., Eldholm, O., 2008. Structure and evolution of the continental margin off Norway and the Barents Sea. Episodes 31, 82-91.

Faleide, J.I., Vågnes, E., Gudlaugsson, S.T., 1993. Late Mesozoic-Cenozoic evolution of the south-western Barents Sea in a regional rift-shear tectonic setting. Mar. Pet. Geol. 10, 186-214.

Fiedler, A., Faleide, J.I., 1996. Cenozoic sedimentation along the southwestern Barents Sea margin in relation to uplift and erosion of the shelf. Global Planet. Change 12, 75-93.

Gabrielsen, R.H., Faerseth, R.B., Jensen, L.N., 1990. Structural Elements of the Norwegian Continental Shelf. Pt. 1. The Barents Sea Region. NPD Bull. 6.

Gibb, J.G., 1978. Rates of coastal erosion and accretion in New Zealand. New Zealand journal of marine and freshwater research 12, 429-456.

Haq, B.U., Hardenbol, J., Vail, P.R., 1987. Chronology of fluctuating sea levels since the Triassic. Science 235, 1156-1167.

Helland-Hansen, W., 2010. Facies and stacking patterns of shelf-deltas within the Palaeogene Battfjellet Formation, Nordenskiöld Land, Svalbard: implications for subsurface reservoir prediction. Sedimentology 57, 190-208.

Helland-Hansen, W., Sømme, T.O., Martinsen, O.J., Lunt, I., Thurmond, J., 2016. Deciphering Earth's Natural Hourglasses: Perspectives On Source-To-Sink Analysis. J. Sediment. Res. 86, 1008-1033.

Henriksen, E., Bjørnseth, H., Hals, T., Heide, T., Kiryukhina, T., Kløvjan, O., Larssen, G., Ryseth, A., Rønning, K., Sollid, K., 2011. Uplift and erosion of the greater Barents Sea: impact on prospectivity and petroleum systems. Geol. Soc., London, Memo. 35, 271-281.

Hjelstuen, B.O., Elverhøi, A., Faleide, J.I., 1996. Cenozoic erosion and sediment yield in the drainage area of the Storfjorden Fan. Global Planet. Change 12, 95-117.

Knies, J., Matthiessen, J., Vogt, C., Laberg, J.S., Hjelstuen, B.O., Smelror, M., Larsen, E., Andreassen, K., Eidvin, T., Vorren, T.O., 2009. The Plio-Pleistocene glaciation of the Barents Sea–Svalbard region: a new model based on revised chronostratigraphy. Quat. Sci. Rev. 28, 812-829.

Knutsen, S.-M., Augustson, J.H., Haremo, P., 2000. Exploring the Norwegian part of the Barents Sea—Norsk Hydro's lessons from nearly 20 years of experience. Norwegian Petroleum Society Special Publications 9, 99-112.

Knutsen, S.-M., Larsen, K., 1997. The late Mesozoic and Cenozoic evolution of the Sørvestsnaget Basin: A tectonostratigraphic mirror for regional events along the Southwestern Barents Sea margin? Mar. Pet. Geol. 14, 27-54.

Knutsen, S.-M., Skjold, L.-J., Skott, P., 1992. Palaeocene and Eocene development of the Tromsø Basin—sedimentary response to rifting and early sea-floor spreading in the Barents Sea area. Norsk Geol. Tidsskr. 72, 191-207.

Kristensen, T., Rotevatn, A., Marvik, M., Henstra, G.A., Gawthorpe, R.L., Ravnås, R., 2017. Structural evolution of sheared margin basins: the role of strain partitioning. Sørvestsnaget Basin, Norwegian Barents Sea. Basin Res.

Kristoffersen, Y., 1990. On the tectonic evolution and paleoceanographic significance of the Fram Strait gateway, Geological history of the polar oceans: arctic versus antarctic. Springer, 63-76.

Kristoffersen, Y., Talwani, M., 1977. Extinct triple junction south of Greenland and the Tertiary motion of Greenland relative to North America. Geol. Soc. Am. Bull. 88, 1037-1049.

Ktenas, D., Henriksen, E., Meisingset, I., Nielsen, J.K., Andreassen, K., 2017. Quantification of the magnitude of net erosion in the southwest Barents Sea using sonic velocities and compaction trends in shales and sandstones. Mar. Pet. Geol.

Laberg, J., Vorren, T., 1993. A late Pleistocene submarine slide on the Bear Island trough mouth fan. Geo-Mar. Lett. 13, 227-234.

Laberg, J., Vorren, T., 1995. Late Weichselian submarine debris flow deposits on the Bear Island Trough mouth fan. Mar. Geol. 127, 45-72.

Laberg, J., Vorren, T., 1996. The Middle and Late Pleistocence evolution and the Bear Island Trough Mouth Fan. Global Planet. Change 12, 309-330.

Laberg, J.S., Andreassen, K., Knies, J., Vorren, T.O., Winsborrow, M., 2010. Late Pliocene–Pleistocene development of the Barents Sea ice sheet. Geology 38, 107-110.

Laberg, J.S., Andreassen, K., Vorren, T.O., 2012. Late Cenozoic erosion of the high-latitude southwestern Barents Sea shelf revisited. Geol. Soc. Am. Bull. 124, 77-88.

Laberg, J.S., Stoker, M.S., Dahlgren, K.T., de Haas, H., Haflidason, H., Hjelstuen, B.O., Nielsen, T., Shannon, P.M., Vorren, T.O., van Weering, T.C., 2005. Cenozoic alongslope processes and sedimentation on the NW European Atlantic margin. Mar. Pet. Geol. 22, 1069-1088.

Lasabuda, A., Laberg, J.S., Knutsen, S.-M., Safronova, P., 2018. Cenozoic tectonostratigraphy and pre-glacial erosion: A mass-balance study of the northwestern Barents Sea margin, Norwegian Arctic. https://doi.org/10.1016/j.jog.2018.03.004

Leeder, M.R., 2009. Sedimentology and sedimentary basins: from turbulence to tectonics. John Wiley & Sons.

Lundin, E., Doré, A., 2002. Mid-Cenozoic post-breakup deformation in the 'passive'margins bordering the Norwegian–Greenland Sea. Mar. Pet. Geol. 19, 79-93.

Lundin, E.R., Doré, A.G., 2011. Hyperextension, serpentinization, and weakening: A new paradigm for rifted margin compressional deformation. Geology 39, 347-350.

Matthews, K.J., Maloney, K.T., Zahirovic, S., Williams, S.E., Seton, M., Müller, R.D., 2016. Global plate boundary evolution and kinematics since the late Paleozoic. Global Planet. Change 146, 226-250.

Milliman, J.D., Meade, R.H., 1983. World-wide delivery of river sediment to the oceans. J. Geol., 1-21.

Mitchum Jr, R., Vail, P., Thompson III, S., 1977. Seismic stratigraphy and global changes of sea level: Part 2. The depositional sequence as a basic unit for stratigraphic analysis: Section 2. Application of seismic reflection configuration to stratigraphic interpretation.

Müller, R.D., Seton, M., Zahirovic, S., Williams, S.E., Matthews, K.J., Wright, N.M., Shephard, G.E., Maloney, K.T., Barnett-Moore, N., Hosseinpour, M., 2016. Ocean basin evolution and global-scale plate reorganization events since Pangea breakup. Annu. Rev. Earth. Planet. Sci 44, 107-138.

Nøttvedt, A., Berglund, L., Rasmussen, E., Steel, R., 1988. Some aspects of Tertiary tectonics and sedimentation along the western Barents Shelf. Geol. Soc., London, Spec. Publ. 39, 421-425.

Perez-Garcia, C., Safronova, P., Mienert, J., Berndt, C., Andreassen, K., 2013. Extensional rise and fall of a salt diapir in the Sørvestsnaget Basin, SW Barents Sea. Mar. Pet. Geol. 46, 129-143.

Petersen, T.G., Hamann, N., Stemmerik, L., 2015. Tectono-sedimentary evolution of the Paleogene succession offshore Northeast Greenland. Marine and Petroleum Geology 67, 481-497.

Prøis, B.M., 2015. Late Paleocene-earliest Eocene prograding system in the SW Barents Sea.

Rachold, V., Grigoriev, M.N., Are, F.E., Solomon, S., Reimnitz, E., Kassens, H., Antonow, M., 2000. Coastal erosion vs riverine sediment discharge in the Arctic Shelf seas. Int. J. Earth Sci. 89, 450-460.

Rasmussen, E., Fjeldskaar, W., 1996. Quantification of the Pliocene-Pleistocene erosion of the Barents Sea from present-day bathymetry. Global Planet. Change 12, 119-133.

Richardsen, G., Vorren, T.O., Tørudbakken, B.O., 1993. Post-Early Cretaceous uplift and erosion in the southern Barents Sea: a discussion based on analysis of seismic interval velocities. Norsk Geol. Tidsskr. 73, 3-20.

Riis, F., Jensen, L.N., 1992. Introduction: measuring uplift and erosion—proposal for a terminology. Norsk Geol. Tidsskr. 72, 223-228.

Ritter, U., Duddy, I.R., Mork, A., Johansen, H., Arne, D.C., 1996. Temperature and uplift history of Bjornoya (Bear Island), Barents Sea. Pet. Geosci. 2, 133-144.

Rydningen, T.A., Høgseth, G., Lasabuda, A., Laberg, J.S., Safronova, P.A., in prep. Origin and sediment budget of an early Neogene - early Quaternary contourite drift system on the SW Barents Sea margin.

Ryseth, A., Augustson, J.H., Charnock, M., Haugerud, O., Knutsen, S.-M., Midbøe, P.S., Opsal, J.G., Sundsbø, G., 2003. Cenozoic stratigraphy and evolution of the Sørvestsnaget Basin, southwestern Barents Sea. Norw. J. Geol. 83, 107-130.

Safronova, P.A., Andreassen, K., Laberg, J.S., Vorren, T.O., 2012. Development and post-depositional deformation of a Middle Eocene deep-water sandy depositional system in the Sørvestsnaget Basin, SW Barents Sea. Mar. Pet. Geol. 36, 83-99.

Sheriff, R.E., 1991. Encyclopedic dictionary of exploration geophysics. 3rd ed. Soc. Expl. Geophys.

Smelror, M., Petrov, O., Larssen, G.B., Werner, S., 2009. Geological history of the Barents Sea. Norges Geol. Undersøkelse, 1-135.

Sættem, J., Bugge, T., Fanavoll, S., Goll, R., Mørk, A., Mørk, M., Smelror, M., Verdenius, J., 1994. Cenozoic margin development and erosion of the Barents Sea: Core evidence from southwest of Bjørnøya. Mar. Geol. 118, 257-281.

Sømme, T.O., Helland-Hansen, W., Martinsen, O.J., Thurmond, J.B., 2009. Relationships between morphological and sedimentological parameters in source-to-sink systems: a basis for predicting semi-quantitative characteristics in subsurface systems. Basin Res. 21, 361-387.

Sømme, T.O., Jackson, C.A.L., 2013. Source-to-sink analysis of ancient sedimentary systems using a subsurface case study from the Møre-Trøndelag area of southern Norway: Part 2–sediment dispersal and forcing mechanisms. Basin Res. 25, 512-531.

Talwani, M., Eldholm, O., 1977. Evolution of the Norwegian-Greenland sea. Geol. Soc. Am. Bull. 88, 969-999.

Tsikalas, F., Eldholm, O., Faleide, J.I., 2002. Early Eocene sea floor spreading and continent-ocean boundary between Jan Mayen and Senja fracture zones in the Norwegian-Greenland Sea. Mar. Geophys. Res. 23, 247-270.

Tsikalas, F., Faleide, J., Eldholm, O., Wilson, J., 2005. Late Mesozoic–Cenozoic structural and stratigraphic correlations between the conjugate mid-Norway and NE Greenland continental margins. Geological Society, London, Petroleum Geology Conference series 6, 785-801.

Vorren, T.O., Richardsen, G., Knutsen, S.-M., Henriksen, E., 1991. Cenozoic erosion and sedimentation in the western Barents Sea. Mar. Pet. Geol. 8, 317-340.

Vågnes, E., Faleide, J., Gudlaugsson, S., 1992. Glacial erosion and tectonic uplift in the Barents Sea. Norsk Geol. Tidsskr. 72, 333-338.

Wood, R., Edrich, S., Hutchison, I., 1989. Influence of North Atlantic Tectonics on the Large-Scale Uplift of the Stappen High and Loppa High, Western Barents Shelf: Chapter 36: North Sea and Barents Shelf. AAPG Mem. 36, 559-566.

Zattin, M., Andreucci, B., de Toffoli, B., Grigo, D., Tsikalas, F., 2016. Thermochronological constraints to late Cenozoic exhumation of the Barents Sea Shelf. Mar. Pet. Geol. 73, 97-104.

Zieba, K.J., Felix, M., Knies, J., 2016. The Pleistocene contribution to the net erosion and sedimentary conditions in the outer Bear Island Trough, western Barents Sea. arktos 2, 23.

Zieba, K.J., Omosanya, K.O., Knies, J., 2017. A flexural isostasy model for the Pleistocene evolution of the Barents Sea bathymetry. Norwegian Journal of Geology/Norsk Geologisk Forening 97.

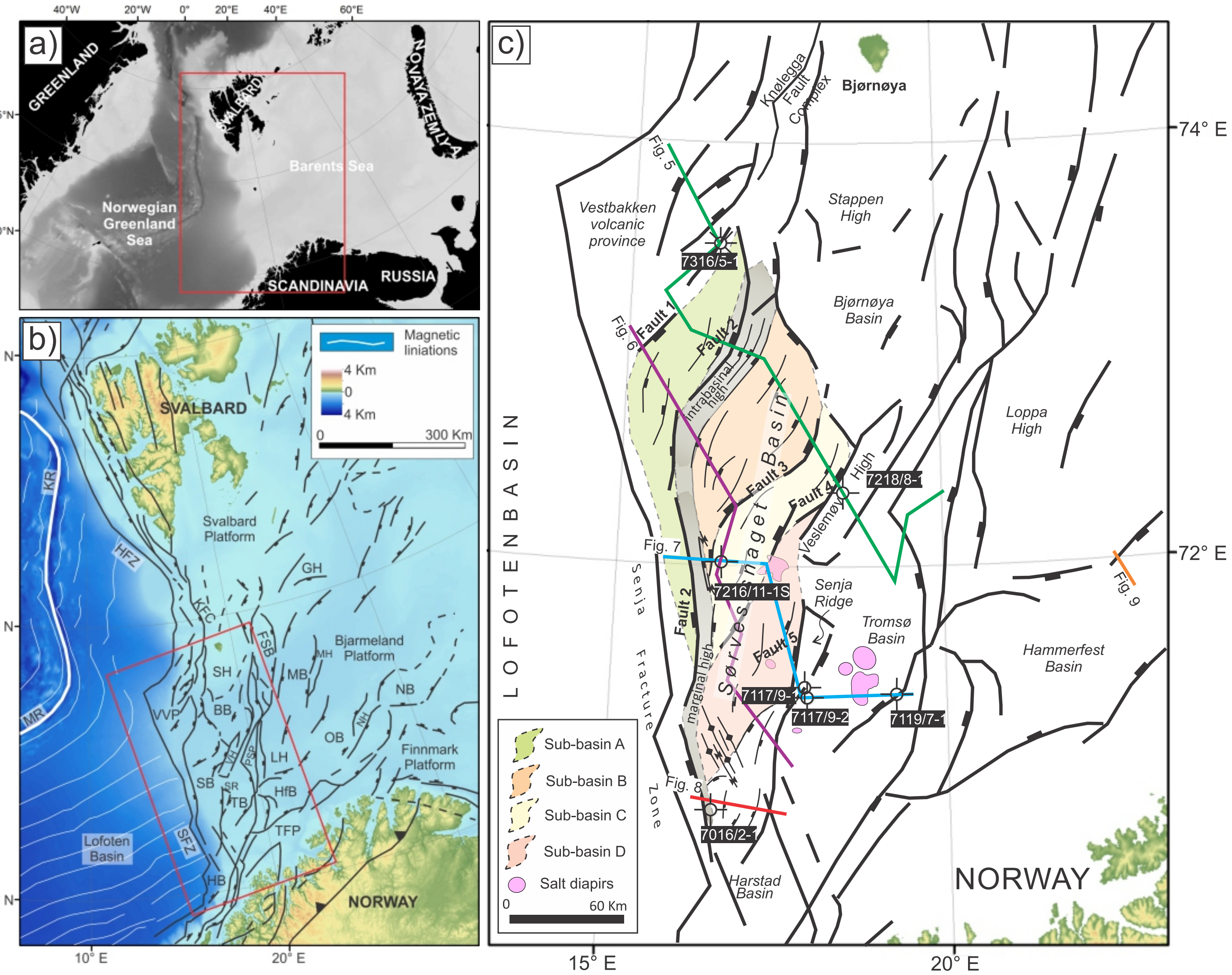

a)
GREENLAND
SVALBARD
NOVAJA ZEMLYA
Barents Sea
Norwegian Greenland Sea
SCANDINAVIA
RUSSIA
b)
Magnetic liniations
4 Km
0
4 Km
0
300 Km
SVALBARD
Svalbard Platform
Bjarmeland Platform
Finnmark Platform
Lofoten Basin
NORWAY
c)
Bjørnøya
Knølegga Fault Complex
Vestbakken volcanic province
Stappen High
Bjørnøya Basin
Loppa High
Veslemøy High
Senja Ridge
Tromsø Basin
Hammerfest Basin
Harstad Basin
Sørvestsnaget Basin
LOFOTEN BASIN
Senja Fracture Zone
Intrabasinal high
marginal high
Fault 1
Fault 2
Fault 3
Fault 4
Fault 5
Fig. 5
Fig. 6
Fig. 7
Fig. 8
Fig. 9
7316/5-1
7218/8-1
7216/11-1S
7117/9-1
7117/9-2
7119/7-1
7016/2-1
Sub-basin A
Sub-basin B
Sub-basin C
Sub-basin D
Salt diapirs
0
60 Km
NORWAY

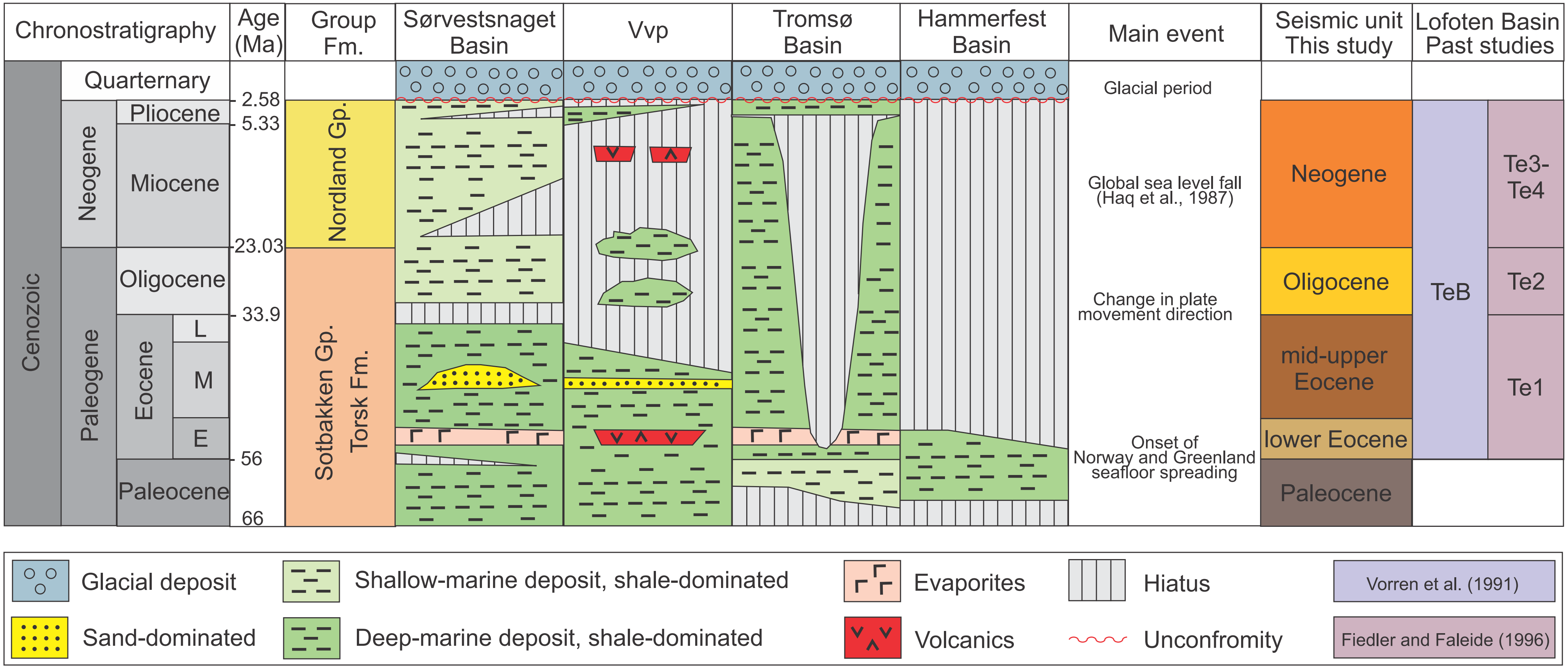

Chronostratigraphy
Age (Ma)
Group Fm.
Sørvestsnaget Basin
Vvp
Tromsø Basin
Hammerfest Basin
Main event
Seismic unit This study
Lofoten Basin Past studies
Cenozoic
Quarternary
Neogene
Pliocene
Miocene
Paleogene
Oligocene
Eocene
L
M
E
Paleocene
2.58
5.33
23.03
33.9
56
66
Nordland Gp.
Sotbakken Gp.
Torsk Fm.
Glacial period
Global sea level fall (Haq et al., 1987)
Change in plate movement direction
Onset of Norway and Greenland seafloor spreading
Neogene
Oligocene
mid-upper Eocene
lower Eocene
Paleocene
TeB
Te3-Te4
Te2
Te1
Glacial deposit
Shallow-marine deposit, shale-dominated
Evaporites
Hiatus
Vorren et al. (1991)
Sand-dominated
Deep-marine deposit, shale-dominated
Volcanics
Unconfromity
Fiedler and Faleide (1996)

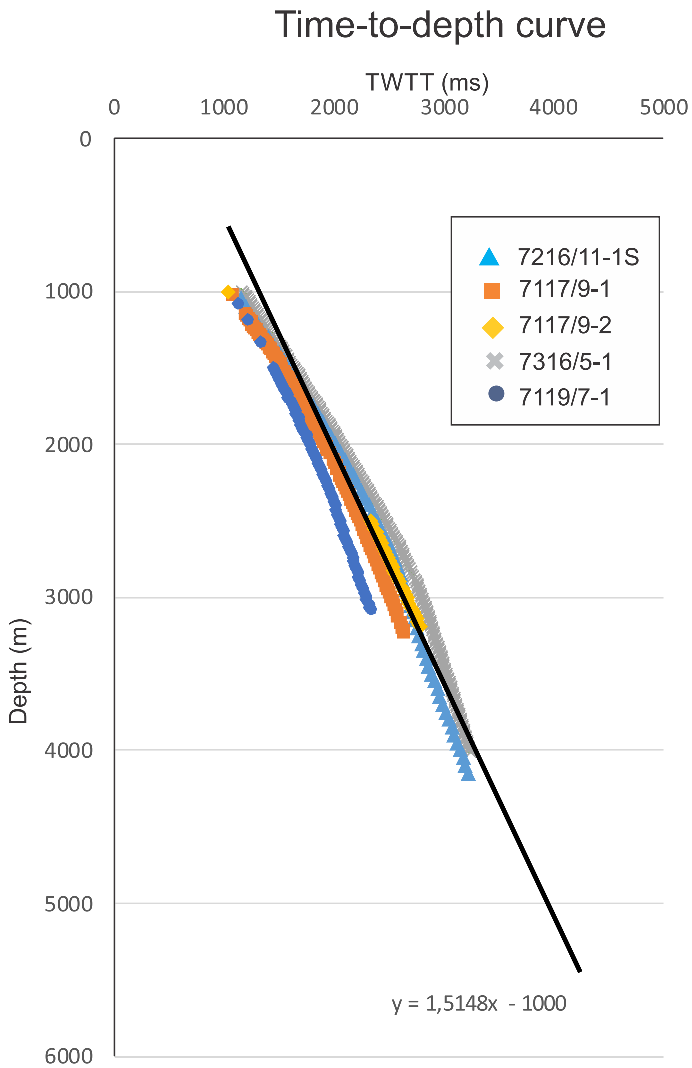

Time-to-depth curve
TWTT (ms)
0
1000
2000
3000
4000
5000
Depth (m)
0
1000
2000
3000
4000
5000
6000
7216/11-1S
7117/9-1
7117/9-2
7316/5-1
7119/7-1
y = 1,5148x - 1000

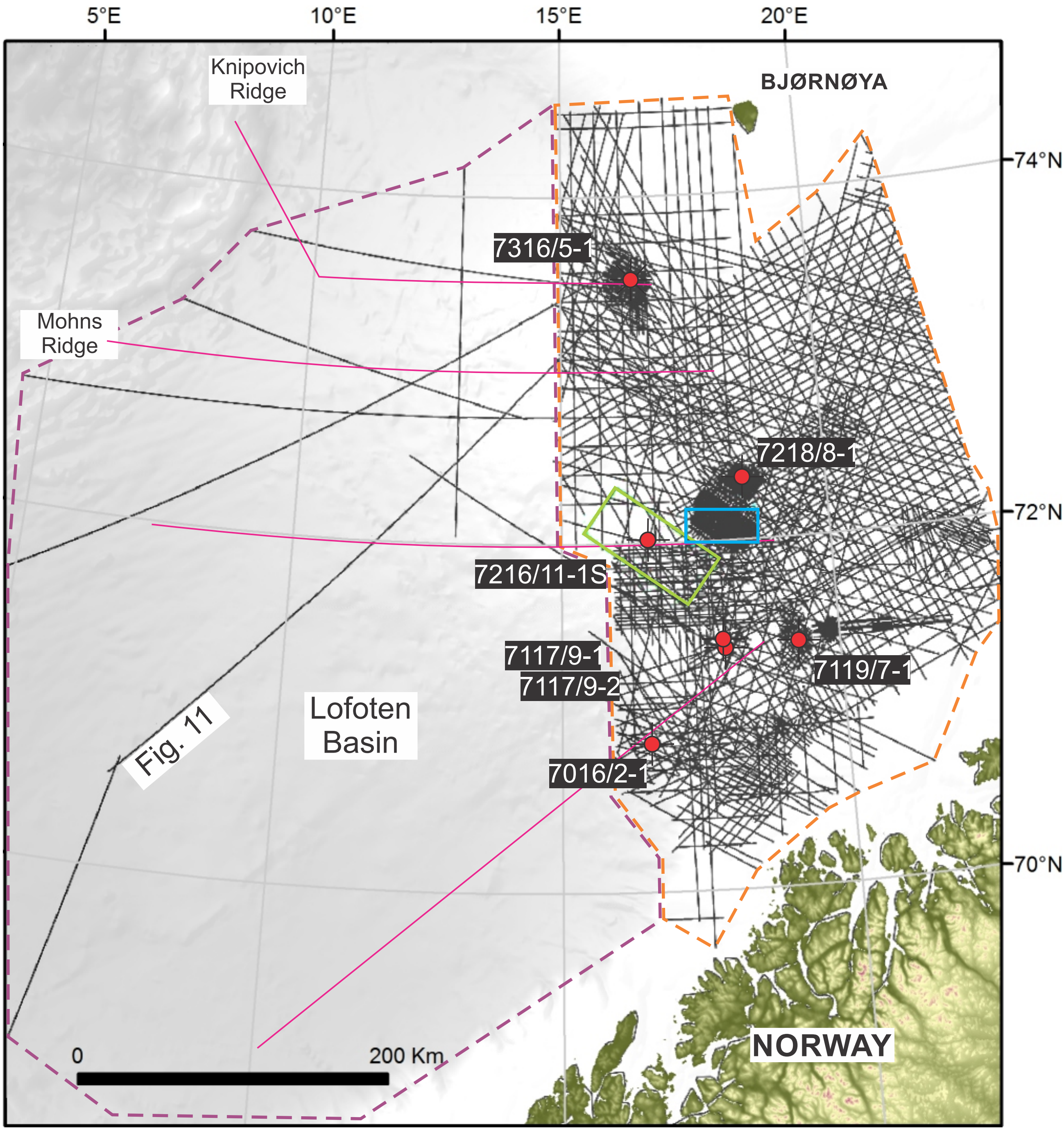
5°E
10°E
15°E
20°E
74°N
72°N
70°N
Knipovich Ridge
BJØRNØYA
7316/5-1
Mohns Ridge
7218/8-1
7216/11-1S
7117/9-1
7117/9-2
7119/7-1
7016/2-1
Fig. 11
Lofoten Basin
0
200 Km
NORWAY

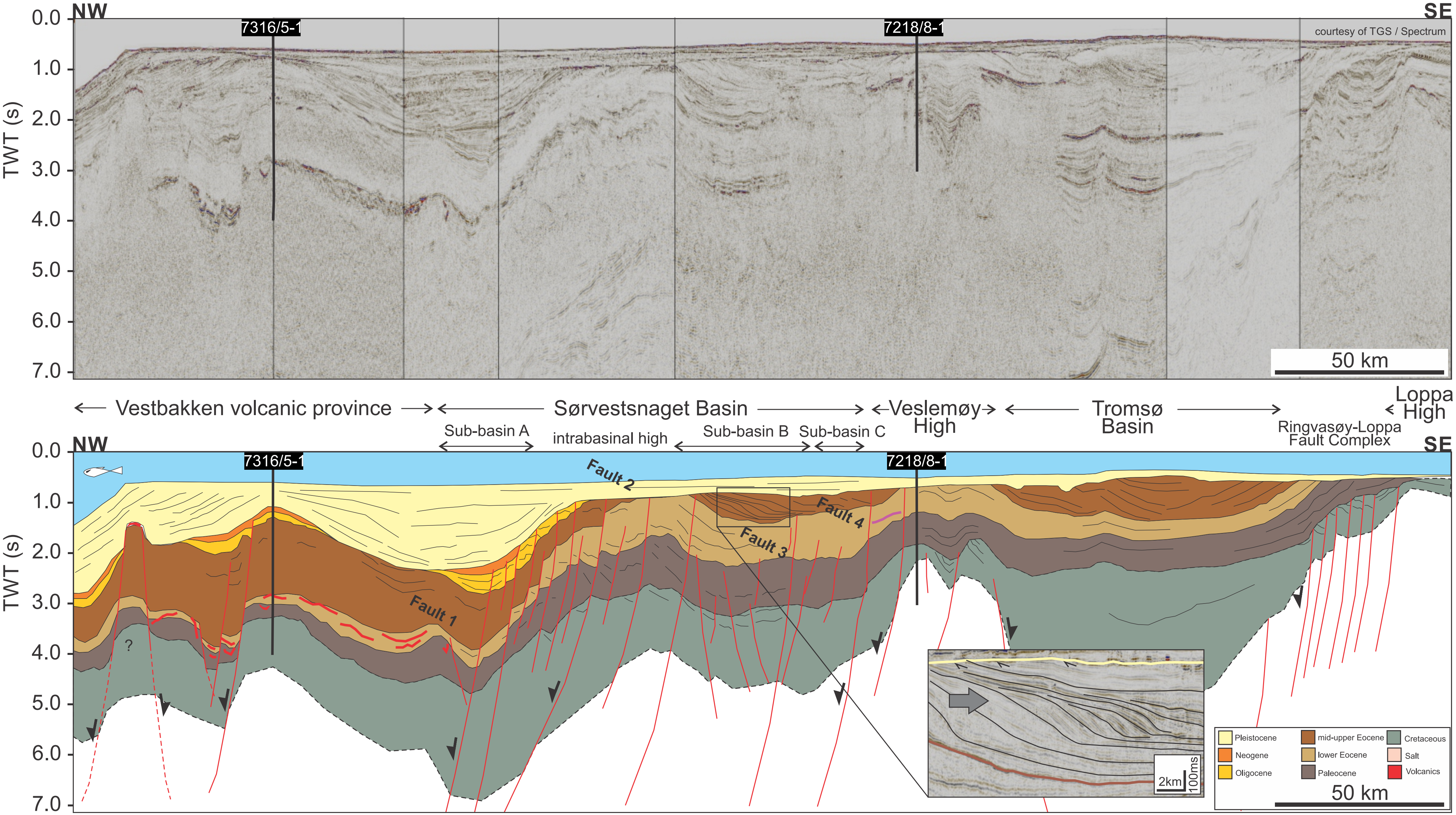

NW
SE
TWT (s)
0.0
1.0
2.0
3.0
4.0
5.0
6.0
7.0
7316/5-1
7218/8-1
courtesy of TGS / Spectrum
50 km
Vestbakken volcanic province
Sørvestsnaget Basin
Veslemøy High
Tromsø Basin
Loppa High
Sub-basin A
intrabasinal high
Sub-basin B
Sub-basin C
Ringvasøy-Loppa Fault Complex
Fault 1
Fault 2
Fault 3
Fault 4
2km
100ms
Pleistocene
Neogene
Oligocene
mid-upper Eocene
lower Eocene
Paleocene
Cretaceous
Salt
Volcanics

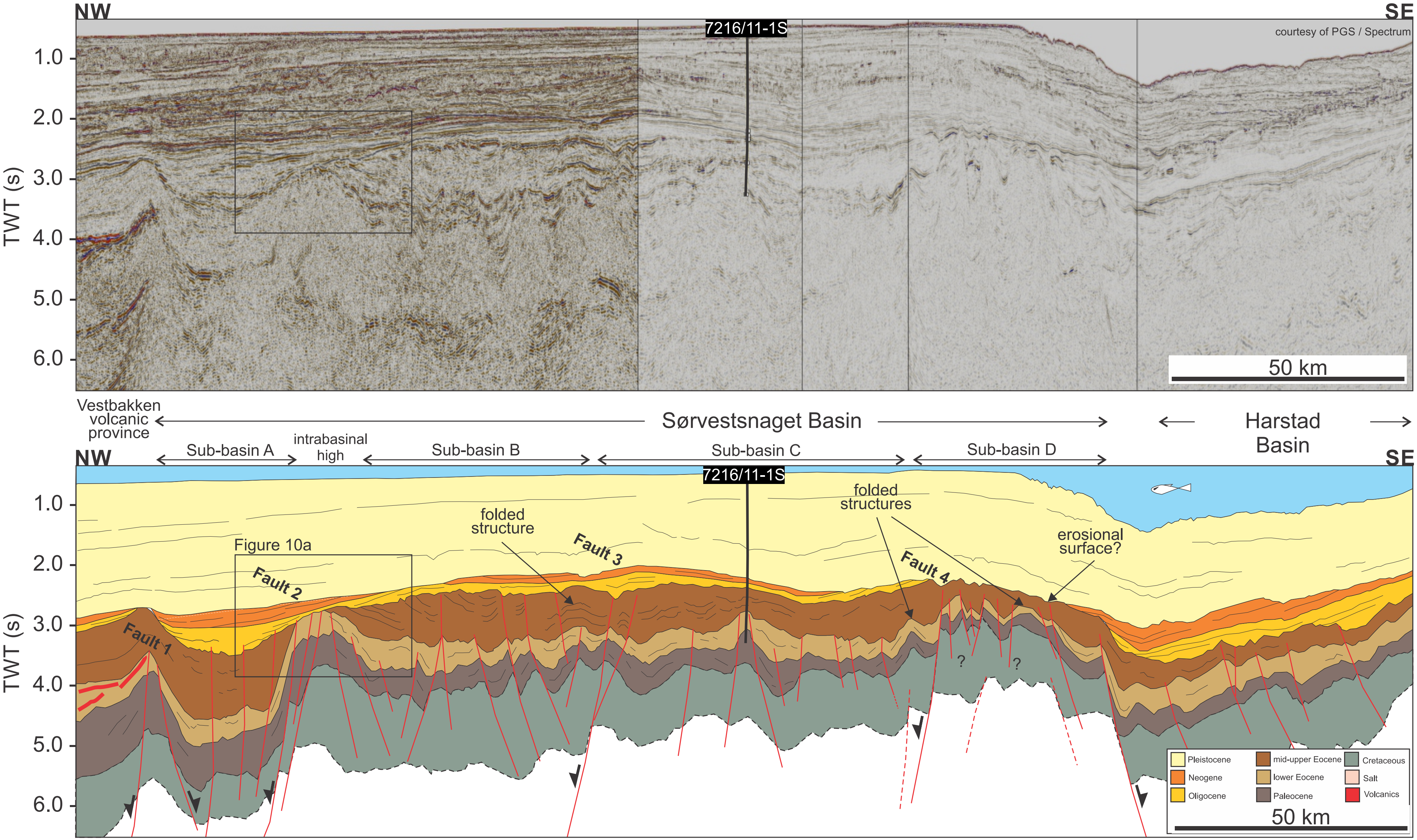

NW
SE
7216/11-1S
courtesy of PGS / Spectrum
TWT (s)
1.0
2.0
3.0
4.0
5.0
6.0
50 km
Vestbakken volcanic province
Sørvestsnaget Basin
Harstad Basin
Sub-basin A
intrabasinal high
Sub-basin B
Sub-basin C
Sub-basin D
NW
SE
7216/11-1S
folded structure
folded structures
erosional surface?
Figure 10a
Fault 1
Fault 2
Fault 3
Fault 4
?
?
Pleistocene
Neogene
Oligocene
mid-upper Eocene
lower Eocene
Paleocene
Cretaceous
Salt
Volcanics
50 km

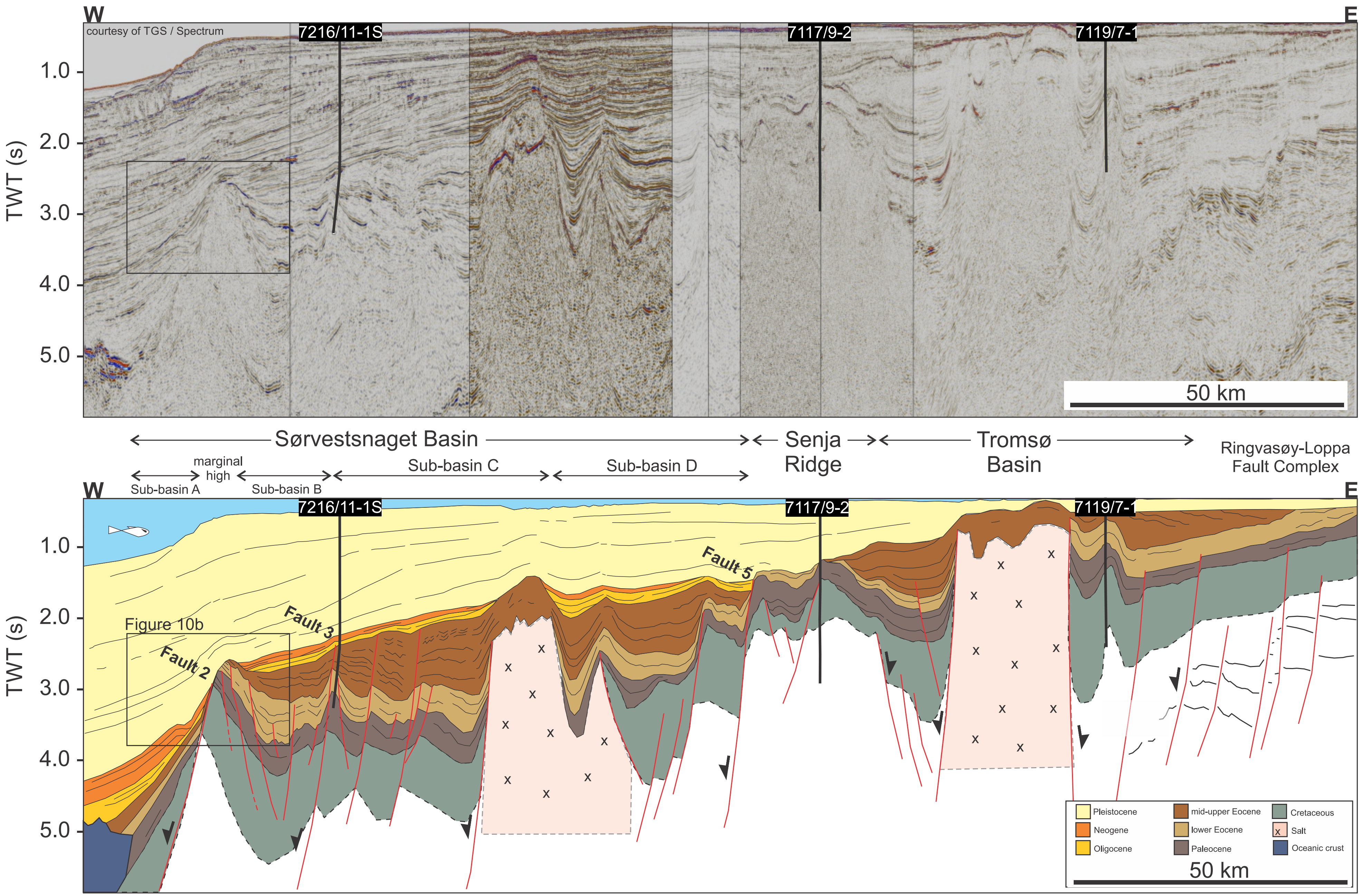

W
E
courtesy of TGS / Spectrum
7216/11-1S
7117/9-2
7119/7-1
TWT (s)
1.0
2.0
3.0
4.0
5.0
50 km
Sørvestsnaget Basin
Senja Ridge
Tromsø Basin
Ringvasøy-Loppa Fault Complex
Sub-basin A
marginal high
Sub-basin B
Sub-basin C
Sub-basin D
Figure 10b
Fault 2
Fault 3
Fault 5
Pleistocene
Neogene
Oligocene
mid-upper Eocene
lower Eocene
Paleocene
Cretaceous
Salt
Oceanic crust

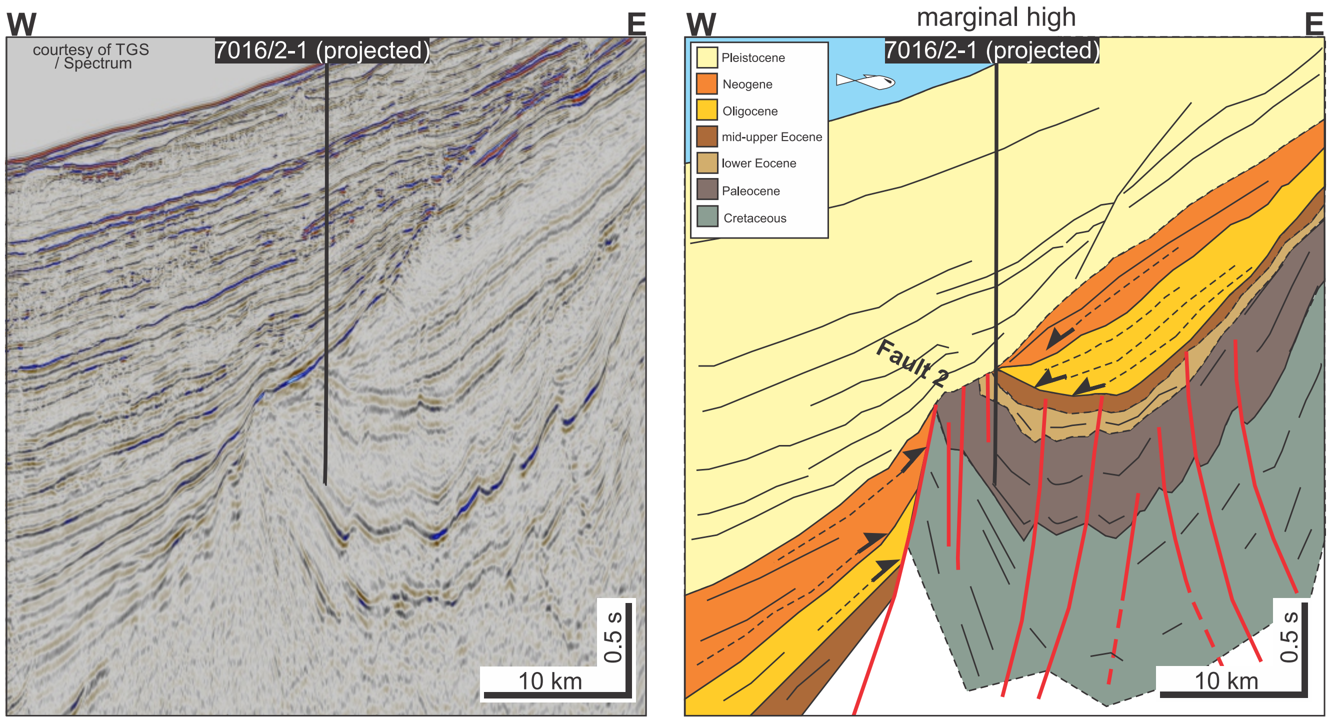
W
E
courtesy of TGS / Spectrum
7016/2-1 (projected)
0.5 s
10 km
W
marginal high
E
7016/2-1 (projected)
Pleistocene
Neogene
Oligocene
mid-upper Eocene
lower Eocene
Paleocene
Cretaceous
Fault 2
0.5 s
10 km

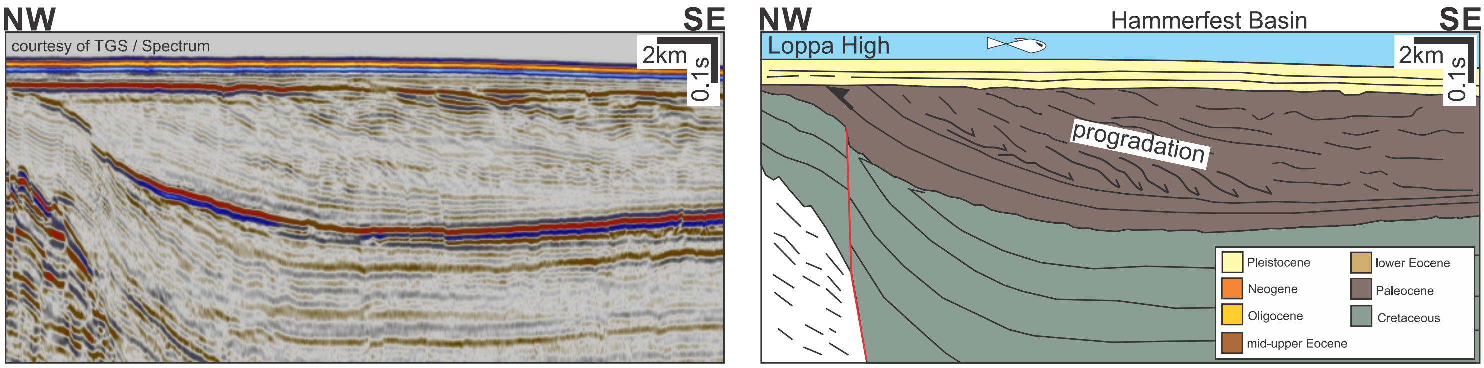
NW
SE
courtesy of TGS / Spectrum
2km
0.1s
NW
Hammerfest Basin
SE
Loppa High
2km
0.1s
progradation
Pleistocene
Neogene
Oligocene
mid-upper Eocene
lower Eocene
Paleocene
Cretaceous

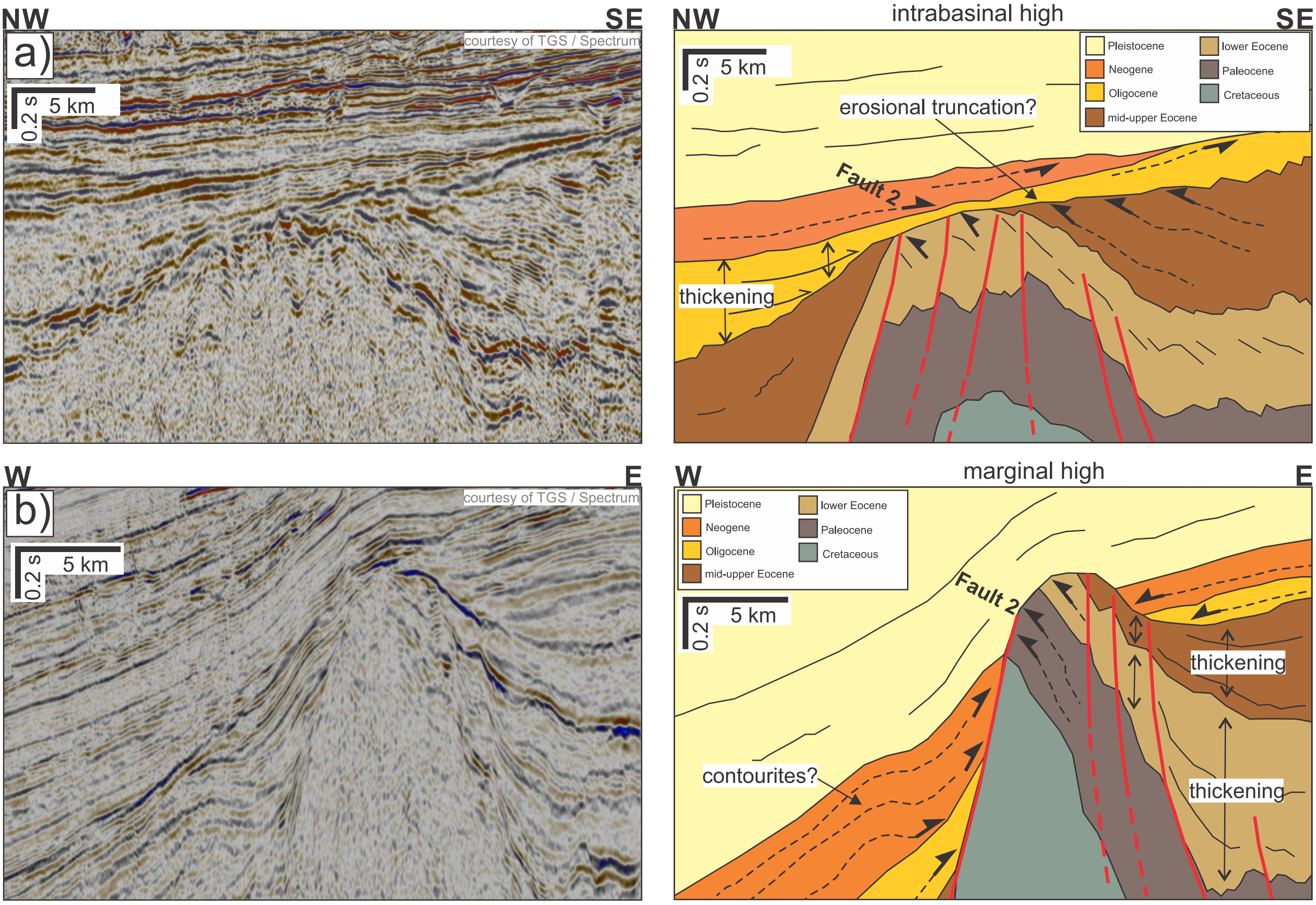

NW
SE
a)
courtesy of TGS / Spectrum
5 km
0.2 s
NW
intrabasinal high
SE
Pleistocene
Neogene
Oligocene
mid-upper Eocene
lower Eocene
Paleocene
Cretaceous
5 km
0.2 s
erosional truncation?
Fault 2
thickening
W
E
b)
courtesy of TGS / Spectrum
5 km
0.2 s
W
marginal high
E
Pleistocene
Neogene
Oligocene
mid-upper Eocene
lower Eocene
Paleocene
Cretaceous
Fault 2
5 km
0.2 s
thickening
contourites?
thickening

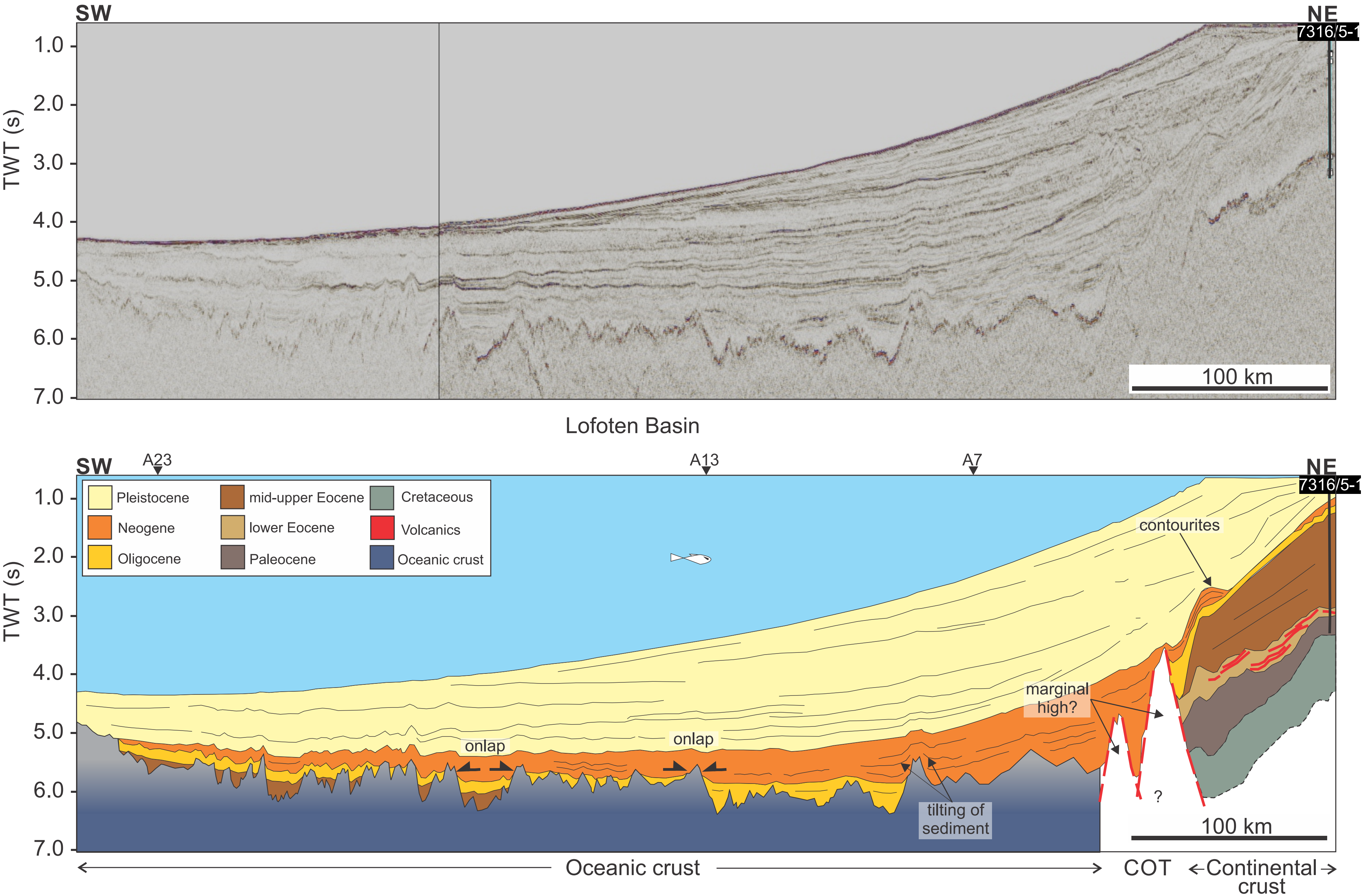

SW
NE
7316/5-1
TWT (s)
1.0
2.0
3.0
4.0
5.0
6.0
7.0
100 km
Lofoten Basin
A23
A13
A7
Pleistocene
Neogene
Oligocene
mid-upper Eocene
lower Eocene
Paleocene
Cretaceous
Volcanics
Oceanic crust
contourites
marginal high?
onlap
onlap
tilting of sediment
?
Oceanic crust
COT
Continental crust

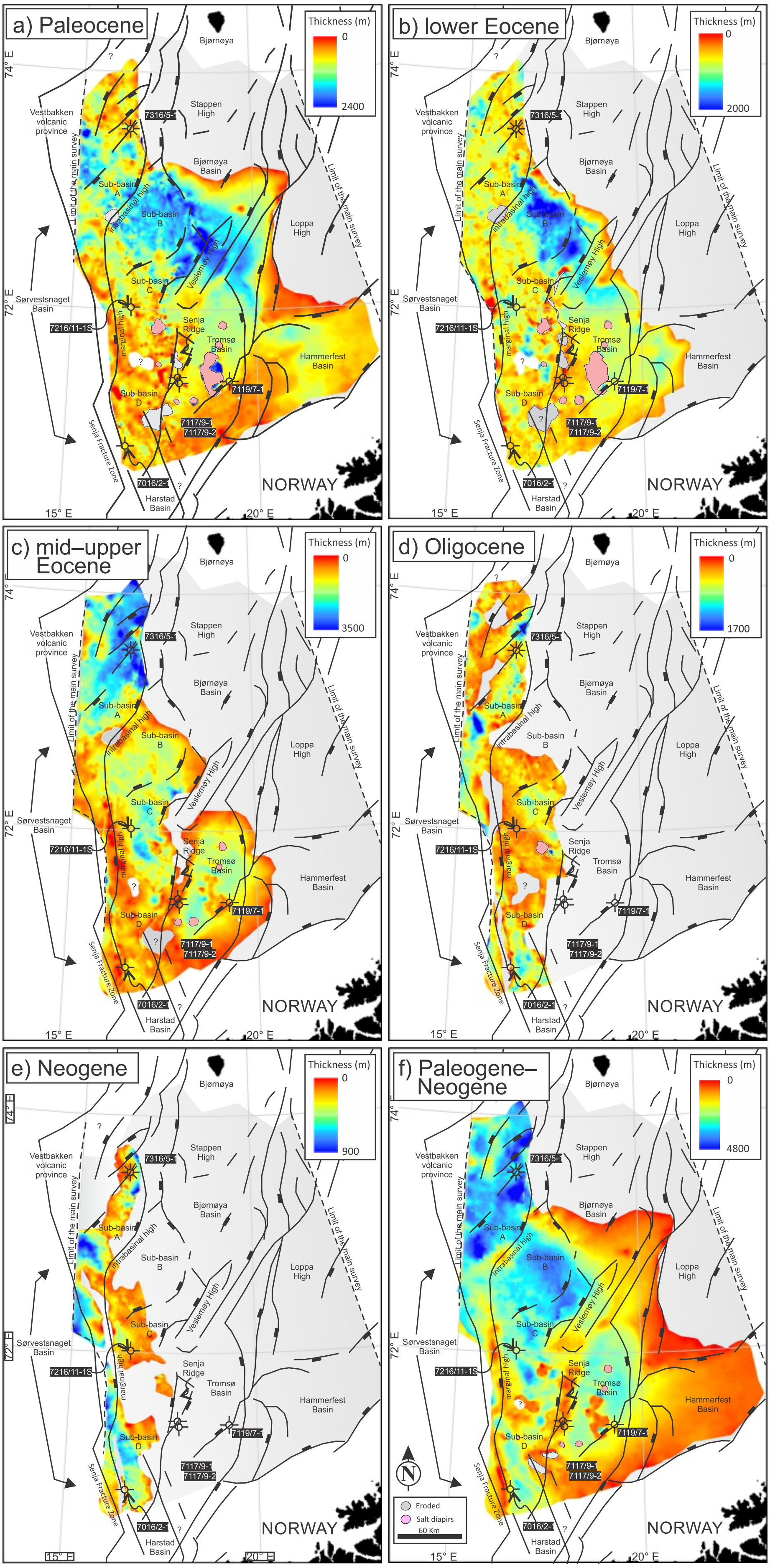
a) Paleocene
Thickness (m)
0
2400
b) lower Eocene
Thickness (m)
0
2000
c) mid–upper Eocene
Thickness (m)
0
3500
d) Oligocene
Thickness (m)
0
1700
e) Neogene
Thickness (m)
0
900
f) Paleogene–Neogene
Thickness (m)
0
4800
Bjørnøya
Stappen High
Bjørnøya Basin
Loppa High
Hammerfest Basin
Tromsø Basin
Senja Ridge
Veslemøy High
Intrabasinal high
Marginal high
Sub-basin A
Sub-basin B
Sub-basin C
Sub-basin D
Vestbakken volcanic province
Sørvestsnaget Basin
Senja Fracture Zone
Harstad Basin
Limit of the main survey
7316/5-1
7216/11-1S
7119/7-1
7117/9-1
7117/9-2
7016/2-1
NORWAY
74° E
72° E
15° E
20° E
Eroded
Salt diapirs
60 Km
N

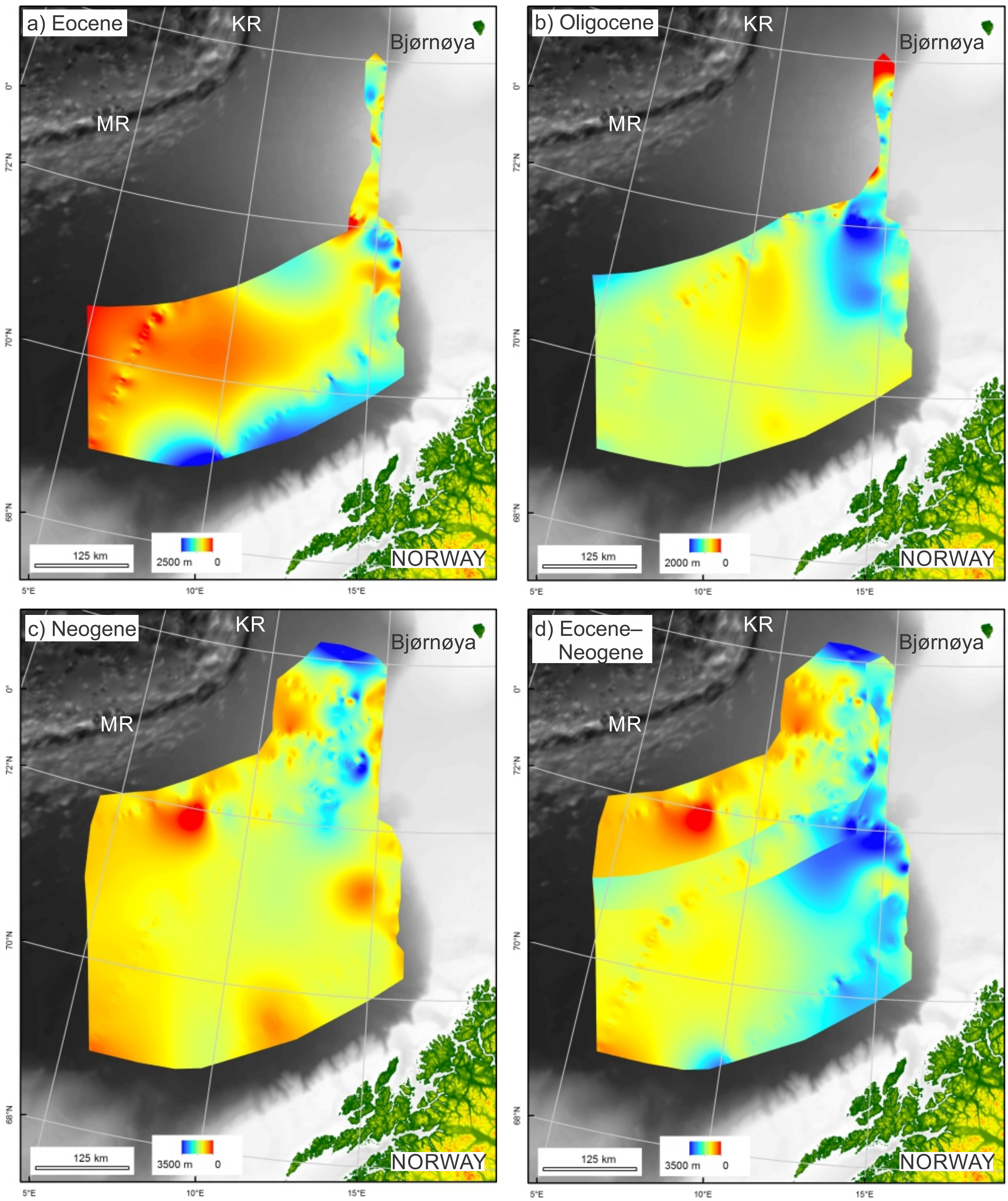
a) Eocene
KR
Bjørnøya
MR
0°
72°N
70°N
68°N
125 km
2500 m
0
NORWAY
5°E
10°E
15°E
b) Oligocene
KR
Bjørnøya
MR
125 km
2000 m
0
NORWAY
c) Neogene
KR
Bjørnøya
MR
125 km
3500 m
0
NORWAY
d) Eocene–
Neogene
KR
Bjørnøya
MR
125 km
3500 m
0
NORWAY

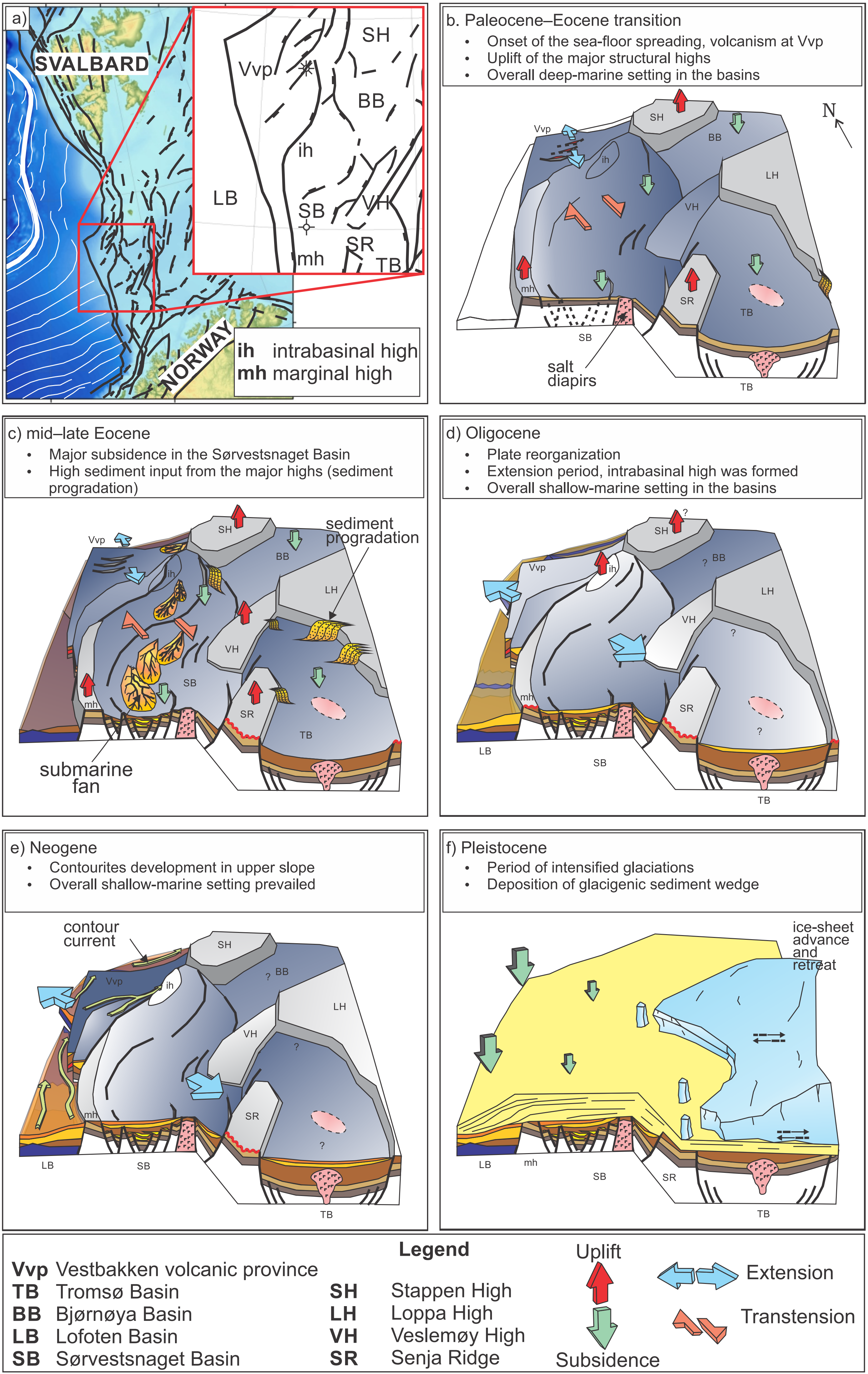

a)
SVALBARD
NORWAY
SH
Vvp
BB
ih
LB
SB
VH
SR
mh
TB
ih intrabasinal high
mh marginal high
b. Paleocene–Eocene transition
• Onset of the sea-floor spreading, volcanism at Vvp
• Uplift of the major structural highs
• Overall deep-marine setting in the basins
N
salt diapirs
c) mid–late Eocene
• Major subsidence in the Sørvestsnaget Basin
• High sediment input from the major highs (sediment progradation)
sediment progradation
submarine fan
d) Oligocene
• Plate reorganization
• Extension period, intrabasinal high was formed
• Overall shallow-marine setting in the basins
e) Neogene
• Contourites development in upper slope
• Overall shallow-marine setting prevailed
contour current
f) Pleistocene
• Period of intensified glaciations
• Deposition of glacigenic sediment wedge
ice-sheet advance and retreat
Legend
Vvp Vestbakken volcanic province
TB Tromsø Basin
BB Bjørnøya Basin
LB Lofoten Basin
SB Sørvestsnaget Basin
SH Stappen High
LH Loppa High
VH Veslemøy High
SR Senja Ridge
Uplift
Subsidence
Extension
Transtension

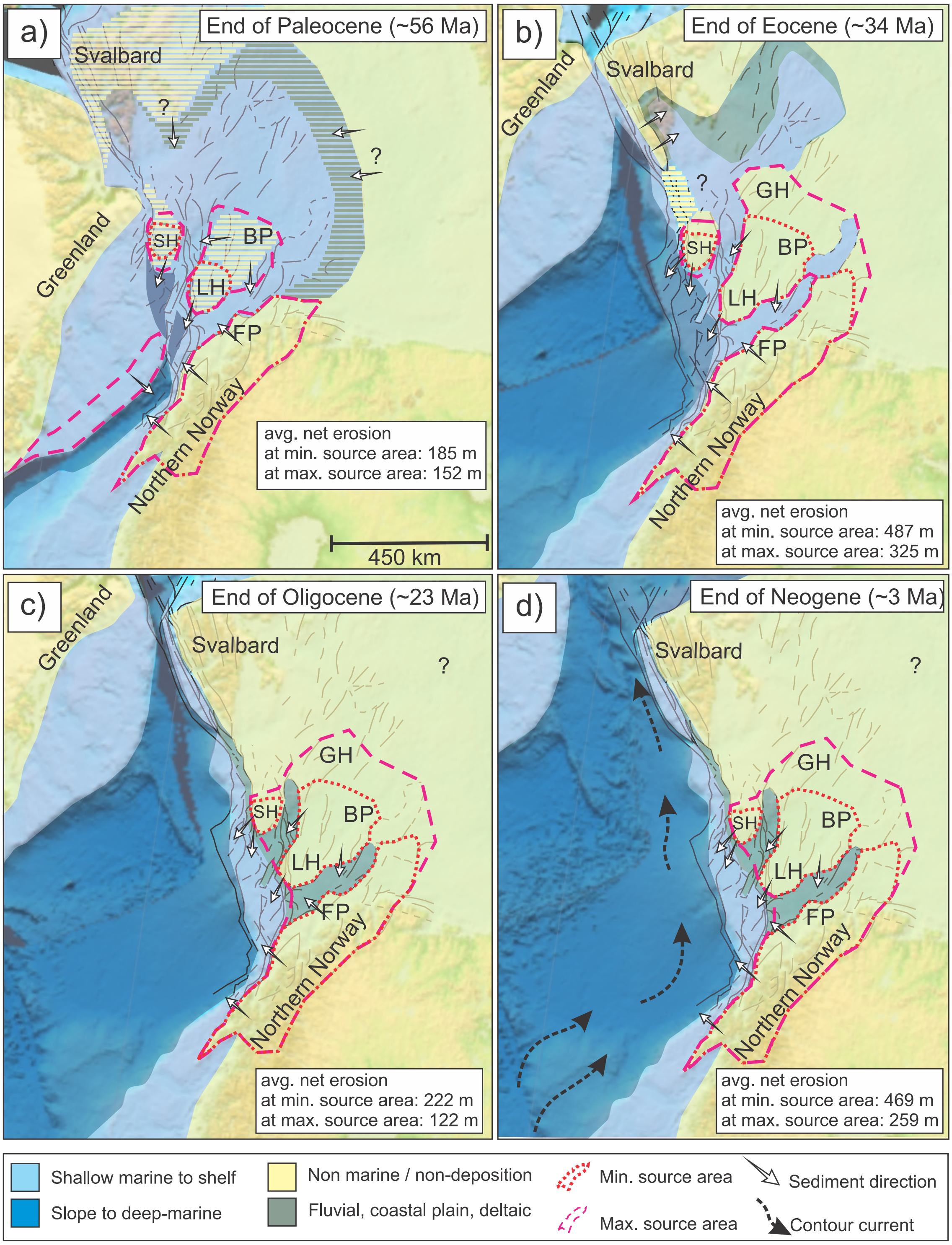
a)
End of Paleocene (~56 Ma)
Svalbard
Greenland
SH
BP
LH
FP
Northern Norway
avg. net erosion
at min. source area: 185 m
at max. source area: 152 m
450 km
b)
End of Eocene (~34 Ma)
Svalbard
Greenland
GH
SH
BP
LH
FP
Northern Norway
avg. net erosion
at min. source area: 487 m
at max. source area: 325 m
c)
End of Oligocene (~23 Ma)
Greenland
Svalbard
GH
SH
BP
LH
FP
Northern Norway
avg. net erosion
at min. source area: 222 m
at max. source area: 122 m
d)
End of Neogene (~3 Ma)
Svalbard
GH
SH
BP
LH
FP
Northern Norway
avg. net erosion
at min. source area: 469 m
at max. source area: 259 m
Shallow marine to shelf
Slope to deep-marine
Non marine / non-deposition
Fluvial, coastal plain, deltaic
Min. source area
Max. source area
Sediment direction
Contour current

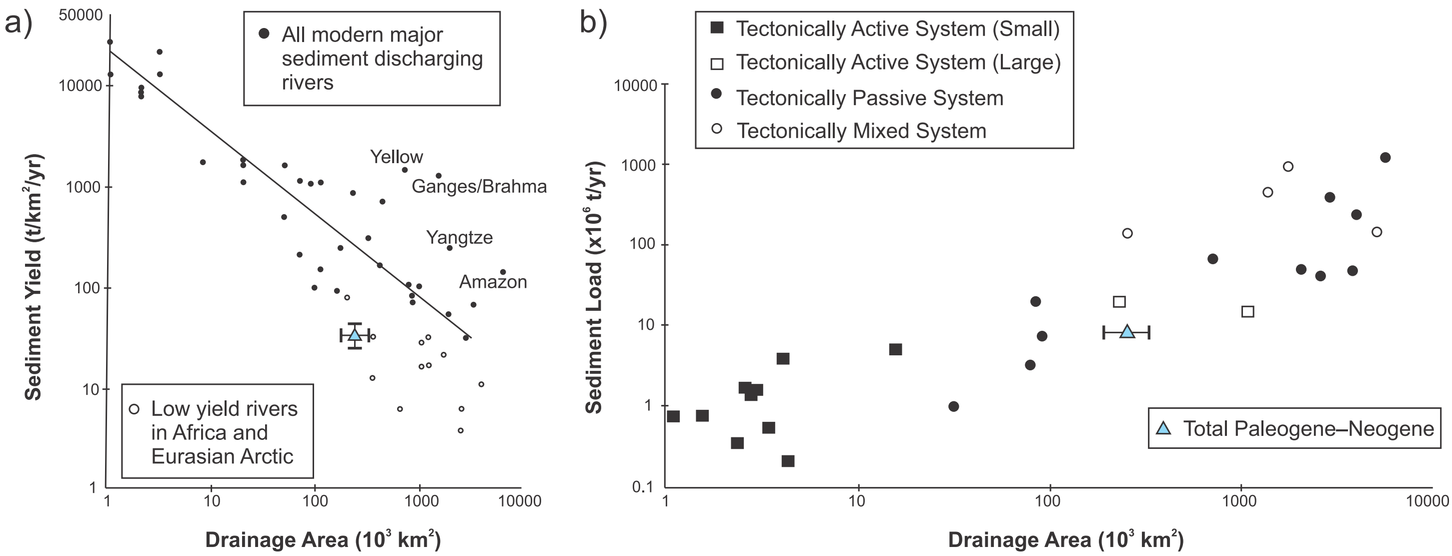
a)
b)
Sediment Yield (t/km²/yr)
Drainage Area (10³ km²)
All modern major sediment discharging rivers
Low yield rivers in Africa and Eurasian Arctic
Yellow
Ganges/Brahma
Yangtze
Amazon
Sediment Load (x10⁶ t/yr)
Tectonically Active System (Small)
Tectonically Active System (Large)
Tectonically Passive System
Tectonically Mixed System
Total Paleogene–Neogene